



Review

A primer on the formation and evolution of hydrogen deficient Central Stars of Planetary Nebulae and Related Objects.

Marcelo M. Miller Bertolami ^{1,2}

¹ Instituto de Astrofísica de La Plata, Consejo Nacional de Investigaciones Científicas y Técnicas Avenida Centenario (Paseo del Bosque) S/N, B1900FWA La Plata; mmiller@fcaglp.unlp.edu.ar

² Facultad de Ciencias Astronómicas y Geofísicas, Universidad Nacional de La Plata Avenida Centenario (Paseo del Bosque) S/N, B1900FWA La Plata, Argentina.

Abstract: We present a brief review on the formation and evolution of hydrogen deficient central stars of planetary nebulae. We include a detailed description of the main observable features of both the central stars and their surrounding nebulae and review their main classifications. We also provide a brief description of the possible progenitor systems of hydrogen deficient central stars, as well as, of transients closely connected to the formation of these stars. In particular we offer a detailed theoretical explanation of the main evolutionary scenarios, both single and binary, devised to explain these stars and nebulae. Particular emphasis is made in the description of the so-called born again scenario, their quantitative predictions and uncertainties. Finally we discuss the pros and cons of both binary and single evolution channels, draw some conclusions and discuss open questions in the field.

Keywords: Planetary Nebula, post-AGB stars, Stellar Evolution

1. Introduction: Planetary Nebulae and their central stars

Contrary to widespread belief, the evolution of low-mass stars is far from fully understood. This is especially true with regard to the formation and evolution of Planetary nebulae (PNe) and their central stars (CSPNe). Discovered in 1764 by Messier [1], our current understanding of PNe was initially drafted by the middle of the twentieth century when it was suggested [2] that CSPNe could be the immediate progenitors of white dwarf (WD) stars, and the descendants of red giants [3]. This scenario received a strong theoretical foundation from numerical stellar evolution models [4,5]. These models showed that, if the envelope of giant stars is removed by very strong winds, the bare nuclei of red giants evolve through of the regions of the Hertzsprung-Russell diagram (HR) corresponding to the CSPNe, and in the appropriate timescales (i.e. tens of thousands of years). Later, several authors [6,7] developed a concrete mechanism involving the interaction between the slow and dense wind of the asymptotic giant branch (AGB) star and the fast and tenuous wind of the CSPNe that explained the global characteristics of PNe. These theoretical studies solidified the idea that CSPNe and their PNe are transition objects between the AGB and the WD cooling sequence.

By the beginning of the twenty-first century the diversity of PNe morphologies together with the discovery of of close binaries in the nuclei of some PNe suggested that binarity might also be involved in the formation and/or shaping of PNe [8–12]. Searches for companions through photometric monitoring and spectroscopic studies have been carried out for decades. Bond [8] reported that 10% to 15% of a sample of about a hundred CSPNe had companions with periods of less than 3 days, which corresponds to what is expected in systems that went through a common envelope phase. Subsequent studies showed an absence of systems with longer periods [13,14]. Using data from the Kepler space telescope, a fraction of close binaries in PNe of 23.5% was derived, with periods between 2 hours and 30 days (almost all of them below 5 days [15]). Photometric searches for cold companions

arXiv:2411.18035v1 [astro-ph.SR] 27 Nov 2024



Citation: Miller Bertolami, M. M. A primer on the formation and evolution of hydrogen deficient Central Stars of Planetary Nebulae and Related Objects.. *Galaxies* 2024, 1, 0. <https://doi.org/>

Received:
Revised:
Accepted:
Published:



Copyright: © 2024 by the author. Licensee MDPI, Basel, Switzerland. This article is an open access article distributed under the terms and conditions of the Creative Commons Attribution (CC BY) license (<https://creativecommons.org/licenses/by/4.0/>).

using infrared excesses [16] determined a fraction of possible companions of $32 \pm 16\%$ or $52 \pm 24\%$ using the I and J bands respectively. This determination includes distant companions that will never interact with the primary. The detection and confirmation of long period binaries is intrinsically complicated due to the large periods involved, which is why they have only recently started to be discovered. There are, currently, only 5 known PNe with measured long period binaries, with periods between 140 and 5000 days and eccentricities between 0 and 0.5¹ [12]. In addition, there are about 12 confirmed binary CSPNe with separations between 90 and 2500 AU. Triple CSPNe are rare but possible. To date only one of these systems (NGC 246) has been confirmed as a triple system [17] while two others (LoTr 5 and Sp 3) have been proposed but not confirmed. Even rarer, observations with the James Webb Space Telescope (JWST) of the PN NGC 3132 suggest that this system might harbour at least a stellar quartet [18]. A separate comment is warranted for the central stars where both components are compact objects (double degenerate systems) in a very close binary, which have been suggested as possible Type Ia SN progenitors. To date only few systems have been studied in detail and all of them have total masses below the Chandrasekhar mass [19–22].

The formation of PNe not only requires material ejection mechanisms able to account for the morphological variety observed but, above all, it requires the synchronization of the time scale associated with the expansion and dissipation of the ejected material, and the time scale associated with the contraction and heating of the central star (CS) that provides the UV photons [e.g. 23]. A direct consequence of this is that not all stars that eject their envelope (either by winds or binary interaction), and contract to form white dwarfs, will form planetary nebulae.

The enormous diversity, not only of morphologies of the PNe but of chemical compositions of both PNe and their CSs suggests that many different evolutionary paths seem to be able to form PNe. More detailed descriptions of the topics covered here and on the various uses and interests of PNe for other areas of the astrophysics can be found in reviews [24] and books [12,25].

In this review we will focus on hydrogen(H)-deficient CSPNe and their planetary nebulae and discuss our current understanding of their formation and evolutionary connections. The paper is organized as follows In section 2 we describe the observed properties and classifications of both H-deficient CSPNe, and the subset of PNe that show H-deficient ejecta. Then, in Section 3 we discuss the so-called born again scenario for the formation of H-deficient CSPNe, and discuss its successes and shortcomings. Here we review different classifications and flavors of the born again scenario, and discuss their predicted chemical abundances. Given their importance in the validation of the born again scenario, in Appendix A we provide a detailed discussion of the properties of confirmed bona fide born again stars. Having discussed the problems with the classical born again scenario we discuss, in Section 4, possible binary evolutionary channels for the formation of H-deficient CSPNe and discuss their own limitations. We close the review with some final comments in Section 5.

2. Hydrogen deficient CSPNe and PNe

2.1. Hydrogen deficient CSPNe

While the majority of CSPNe maintain their original H-rich surface composition, the study of CSPNe exhibiting emission-line spectra, which are very similar to those of massive Wolf-Rayet stars with strong helium (He) and carbon (C) emission lines (i.e., spectral types [WC] and [WO]²), suggested the existence of H-deficient CSPNe stars [27–29]. Later, the

¹ A regularly updated database is available on David Jones' website <https://www.drdjones.net/bcspn/>

² The use of square brackets was proposed by [26] to distinguish the Wolf-Rayet CSPNe from their massive counterparts. [WC] stars are also divided into "late" (cool, spectral classes [WC 6]-[WC 12]) and "early" (hot, spectral classes [WC 4]-[WC 5]) spectral types and denoted by [WCL] and [WCE] respectively. All [WO] stars have "early" spectral types (spectral classes [WO 1]-[WO 4]). In this paper we use [WCE] to include both [WC 4]-[WC 5] and [WO1]- [WO 4] spectral classes.

Palomar-Green survey revealed a new spectral class of H-deficient stars, some of which are CSPNe, the PG1159 stars, which are dominated by absorption lines of highly ionized He, C, and O [30]. It is currently understood that a sizable minority between one fifth and one third of all CSPNe show a strong H-deficient surface composition [31]. The majority of these H-deficient CSPNe exhibit spectra with strong C and He lines. Quantitative spectral analysis of these stars determined that their surface is composed predominantly by these elements [32–36]. In addition to He and C, both PG1159, [WC] and [WO] stars show an important presence of oxygen(O). A couple of objects have been discovered that display spectral characteristics intermediate to that of PG1159 and [WC] spectral types, these stars are sometimes labeled as [WC]-PG1159 [37]. Two well studied cases of [WC]-PG1159 are the CS of Abell 30 and Abell 78, both which have been previously linked to the so-called born again scenario ([38,39], see Section 3). The qualitatively similar He, C and O abundances suggest that all these spectral types might be evolutionary connected. Fig. 1 show the typical surface luminosity and and effective temperatures of different types of H-deficient CSPNe taken from [31] together with the evolutionary tracks of born again models (see Section 3).

In addition to the C-rich H-deficient group mentioned above, a minority of H-deficient CSPNe show He-dominated atmospheres, with traces of nitrogen (N). The spectra of these stars is mostly defined by an almost pure He II absorption-line spectrum in the optical wavelength range [40–42]. The spectral types of these He-dominated CSPNe are O(He), DO WDs, and at least one [WN] (IC 4663, [43]). It is worth noting that not all O(He) are CSPNe, and most DO WDs are not. Due to their He-dominated atmospheres, and the presence of a measurable amount of N, similar to that of the majority of R Coronae Borealis (RCrB) stars and extreme helium stars (EHe) stars [44,45], the He-dominated CSPNe have been linked to RCrB, EHe, and to the occurrence of CO-core WD + He-core WD mergers [46,47].

Besides the previously mentioned groups there is an even smaller group of H-deficient CSPNe that still display significant amounts of H (larger than 10% by mass fraction) and with different spectral types. These are the CSs of Abell 48 ([WN],[48–50]), PB 8 ([WN/C], [51,52], and the CSs of Sh 2-68, Abell 43, and NGC 7094, all classified as “Hybrid PG1159” stars, from now on H-PG1159 stars [37,53]. Good descriptions of the typical abundances in [WR] and PG1159 stars are discussed by [37,54,55].

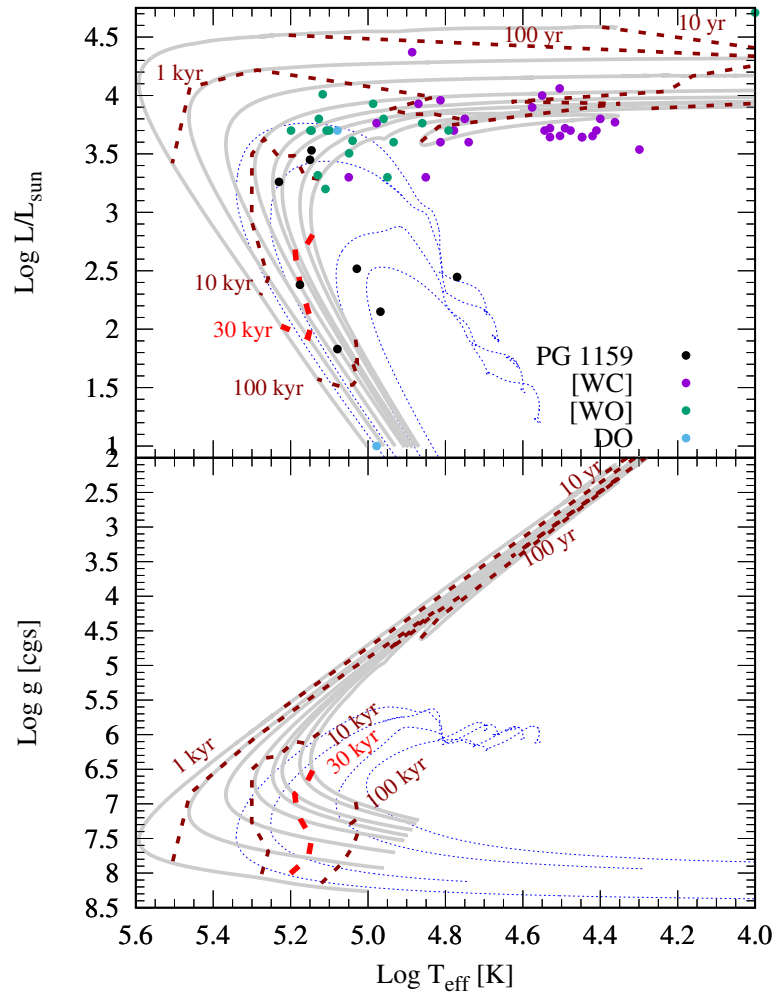


Figure 1. Upper panel: Location of the different H-deficient CSPNe in the HR diagram from the recent catalog of Weidmann et al. [31] together with their spectral types. Note the dearth of [WR] stars at around $T_{\text{eff}} \sim 50000\text{K}$. Grey lines indicate the location and evolution of models of H-deficient CSPNe with their corresponding isochrones (dashed lines) [56–58]. Grey tracks correspond to post-VLTP sequences with remnant masses of (from right to left): 0.53, 0.542, 0.5647, 0.5886, 0.609, 0.6641, 0.7411 and $0.8697 M_{\odot}$. See Section 3.2 for a discussion on the born again scenario and its different flavors. Dotted blue tracks correspond to low-mass post merger models (He-core WD + low-mass CO-core WD) with masses 0.48, 0.55, 0.7 and $0.8 M_{\odot}$ (from right to left). Lower panel: Evolution of the same models shown in the upper panel but in a Kiel diagram.

2.2. Pulsating H-deficient CSPNe (GW Vir)

Some H-deficient CSPNe with PG1159 and [WCE] spectral types belong to a small subgroup of variable stars known as GW Vir, after the prototype of the class PG 1159-035 [59,60]. GW Vir that are surrounded by a PN are also named variable planetary nebula nuclei or PNNVs. GW Vir exhibit multi-periodic lightcurves that are attributed to non-radial pulsations in high radial order g modes of low harmonic degree. The typical pulsation periods observed are in the range of 300s to 3000s, and are explained by the action of the classical $\kappa - \gamma$ mechanism due to partial ionization of C and O, which are extremely abundant in the envelope of these stars [see 61,62, for a detailed discussion]. The existence of multiperiodic lightcurves in these stars opened the possibility to use asteroseismological techniques to study the properties of CSPNe. More specifically asteroseismology offers unparalleled accuracy in the determination of masses [63–69], and might even offer the

opportunity to determine the internal rotation profiles of CSPNe [70,71]. The large number of periods found in GW Vir (usually about 20 frequencies but up to 200 frequencies in the case of PG 1159-035) allows masses to be determined to a precision of a few percent, exceeding what can be determined by spectroscopic means in this complicated regime [72]. Moreover, pulsational properties of GW Vir have the potential to place constraints on the internal structure of PG1159 stars, and, consequently testing the validity of potential formation scenarios. This approach was explored by [73] who tested the possibility of using mode-trapping features in the period spacings of GW Vir to put constraints on the properties of convective boundary mixing (CBM) during the core He burning stage. More concretely [74] found that the mixture of positive and negative rates of change of the periods of the normal modes measured in the prototype star PG 1159-035 can be interpreted as a strong hint that PG1159 stars could be characterized by substantially thinner helium-rich envelopes than traditionally implied by the standard theory of the formation and evolution of PG 1159 stars.

2.3. Hydrogen deficient PNe

Almost all PNe have chemical compositions dominated by H with traces of other chemical elements [24]. There exists, however, a small group for which regions of H-deficient (He-dominated) material have been discovered [75]. These PNe are commonly termed "born again PNe" for the suspected connection with the born again stars³. To the best of our knowledge the group of PNe with known H-deficient inner regions includes: Abell 30 [76], Abell 78 [77], Abell 58 [78], IRAS 18333-2357 [79,80], IRAS 15154-5258 [81], the PNe around V4334 Sgr (a.k.a. Sakurai's Object) [82], WR 72 [83], and HuBi 1 [84]. All these H-deficient PNe for which the CS has been spectroscopically studied harbor in their center a H-deficient CS, which indicates beyond reasonable doubt that a single event is responsible for both deficiencies in H. Besides the common nature of their CSs these born again PNe also share many other characteristics. Most importantly in almost all these PNe the outer H-rich PN is old, circular (or near-spherical), and expanding at normal speeds while the inner H-deficient regions expand much faster, have axisymmetrical shapes (disks and/or bipolar outflows), and display clear cometary knots [75,84–94]⁴. Another interesting feature in H-deficient PNe comes from the so-called abundance discrepancy factors (ADFs⁵). Although, to the best of our knowledge, the only H-deficient PNe with measured ADFs are Abell 30 and Abell 58, values are very high in both cases. ADFs of 90 have been found for Abell 58 [97] and, even higher values were derived for some H-deficient knots in Abell 30 (22, for J4 [98], 600 for J3, and 770 for J1 [99])⁶. This feature is interesting both for the study of H-deficient PNe and of ADFs. In particular, a strong connection have been found, in standard PNe, between very high ADFs and the binarity of their central stars [100]. Although it should be noted that the presence of H-deficient inclusions has also been proposed as an explanation for high ADFs [101]. Regarding the possible binary nature of the CS of the 8 known H-deficient PNe described in this section, only for Abell 30 the possibility of a close binary CS has been suggested through the study of light curve brightness variations [102].

³ Note that the term born again PNe is misleading, as during a born again event (section 3) the evolution of the central star might be fast enough so that the original PNe never "dies". This is actually what has been observed in Abell 58 (see Appendix A) where the CS returned to very high effective temperatures well before the old PNe disappeared. Originally the term born again was coined with the idea of the rebirth of the central star [39].

⁴ An exception to this case might be old PNe around HuBi 1 for which Guerrero et al. [95] reported a barrel-like structure with faint polar protrusions.

⁵ ADFs consists in the discrepancy found in ionized nebulae when deriving abundances from recombination lines and collisionally excited lines [96]. Typical values of the ADFs are around 2 to 3 in PNe [24].

⁶ A compilation PNe with measured ADFs is available on Roger Wesson's website <https://nebulousresearch.org/adfs/>

3. The Born Again Scenario

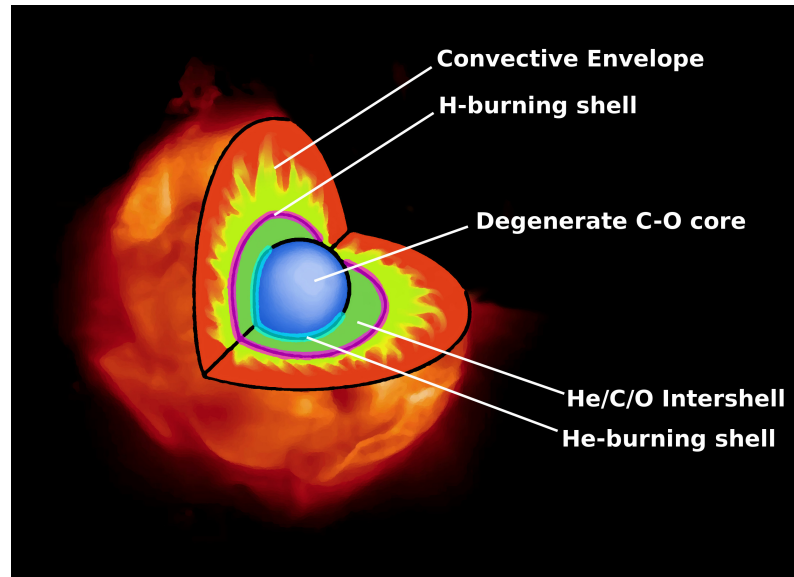


Figure 2. Schematic diagram of the internal structure of an AGB star. Note that for the sake of clarity the diagram is severely not to scale. While outer convective envelope has a radius of the order of the Sun-Earth distance, the degenerate CO-core has a size comparable to that of Earth, and the outer He/C/O intershell has a size similar to that of the icy planets of the Solar System.

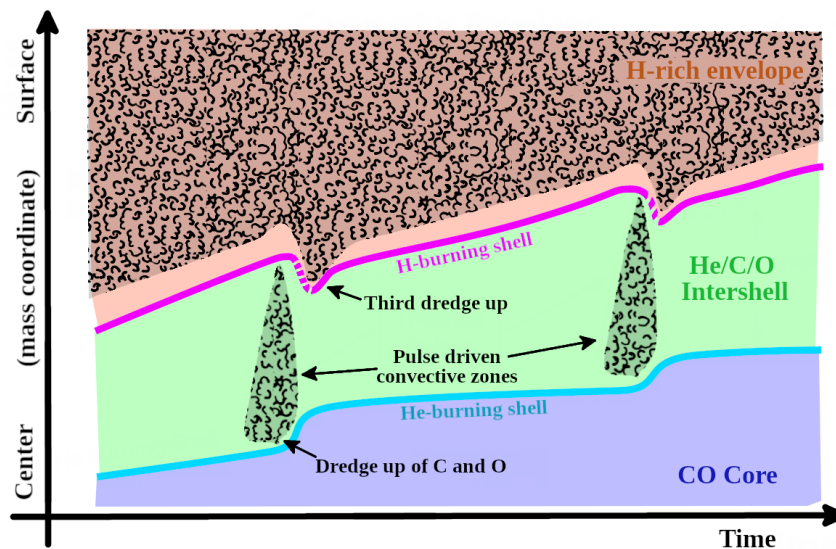


Figure 3. Schematic Kippenhahn diagram of the internal structure of an AGB star during the thermal pulses. Colors are similar to those of Fig.2.

3.1. The thermal pulses on the AGB

One of the most accepted scenarios for the formation of H-deficient CSPNe and WDs is the so-called born again scenario [38,39]. In order to understand the essence of the born again scenario, here we provide a brief description of the immediate progenitors of those stars. We refer the reader to [103] for a detailed explanation of the evolution of single low- and intermediate-mass stars. Fig. 2 shows the internal structure of both low- and intermediate-mass stars when they reach the AGB. After burning H in the center during the main sequence, and then burning He in the center, these stars have a well-layered structure. At the center of this structure lies a CO core supported by the pressure of degenerate

electrons, which is surrounded by a He-burning shell. Above the He-burning shell there is an intershell region rich in He, C and O, on top of which sits a H-burning shell, where H is transformed into He by the CNO cycle. Finally, the H burning shell is surrounded by an envelope composed mostly of unprocessed H and He, which is what gives the AGB star its giant size.

The importance of the structure of AGB stars for the study of H-deficient CSPNe lies in the fact that, at the end of the AGB, the He-burning shell experiences a series of instabilities where the energy released is temporarily increased by about 5 orders of magnitude, or even more [104]. These instabilities are called thermal pulses (or He-shell flashes) and have, as one of their most direct consequences, the development of convective instabilities in the stellar interior (the so-called pulse driven convective zone, PDCZ). Fig. 3 displays a schematic Kippenhahn diagram (i.e. mass coordinate $m(r)$ vs. time) of this phase. Cloudy regions in Fig. 3 indicate convective regions where material is being mixed. Two main dredge up episodes might take place during this stage. One happens during the thermal pulse itself where the lower boundary of the PDCZ dabbles into the CO core of the star, dredging both C and O to the intershell region. The extent of this mixing depends both on the mass of the CO core and on the treatment of convective boundary mixing (CBM, a.k.a. “overshooting”). More intense CBM leads to larger amounts of C and O being dredged up. In particular the more intense the CBM the larger the O enrichment of the intershell. The other dredge up episode, the so-called third dredge up [105], might happen immediately after the thermal pulse, when the envelope expands reacting to the thermal pulse. There the outer convective zone can penetrate into the He-, C- and O-rich intershell, polluting the H-rich envelope with the material from the intershell. Whether third dredge up occurs or not, again, depends both on the mass of the core and the treatment of CBM, as well as on the metallicity of the star [105]. Low-mass AGB stars (e.g. initially $\sim 1M_{\odot}$ stars, with cores of $\sim 0.53M_{\odot}$) will not experience third dredge up under standard CBM assumptions, while more massive stars will experience progressively stronger third dredge up episodes [105]. Besides enriching the envelope in He, C and O, third dredge up plays a critical role in the production of heavy elements through slow neutron capture process [105]. Conditions at the bottom of the convective envelope during third dredge up episodes allow for the partial mixing of ^{12}C and H, which can later be burned to produce ^{13}C during the interpulse phase. When the next thermal pulse happens ^{13}C will be engulfed by the PDCZ and burnt with He, leading to the creation of free neutrons that can feed the slow neutron capture process.

At the same time the star is undergoing thermal pulses it is subject to very strong winds ($\dot{M} \sim 10^{-8}$ – $10^{-4} M_{\odot}/\text{yr}$). The accepted view of AGB winds is that they are driven by radiation pressure on solid-state particles (dust grains) formed in the outer regions of the AGB atmospheres that are levitated by pulsation. Depending on the composition of the atmosphere these dust particles are either made of silicates (when $\text{C}/\text{O} < 1$ by number) or amorphous carbon (when $\text{C}/\text{O} > 1$ by number). All AGB stars are initially of spectral type M (with $\text{C}/\text{O} \simeq 0.5$ by number), but when third dredge up is active, newly produced carbon may eventually lead to a ratio of $\text{C}/\text{O} > 1$ in the atmosphere (carbon star, spectral type C)⁷. This transition from M-stars into carbon stars can be critical for the AGB winds, as silicate dust is made from elements that are not produced in low-mass stars and consequently winds in this stage will depend on the original metallicity of the star. Conversely, carbon dust is based on primary carbon produced by the AGB star and C-dust driven winds will be mostly independent on the original metallicity of the star. A detailed review of AGB winds and their modeling can be found in [106]. In addition to this, [107] showed that, as soon as the the star becomes a carbon star and carbon rich molecules are formed in the atmosphere, the star becomes cooler and more extended, increasing the intensity of the AGB winds. The main consequence of these strong winds is that the H-rich envelope is finally reduced below the critical mass that allows for a giant configuration. When this happens the star will depart from the AGB and start evolving, first as a post-AGB star,

⁷ In the transition from spectral type M to C, S-stars are formed ($0.5 < \text{C}/\text{O} < 1$)

and latter as a hot pre-WD. If conditions are appropriate a PN can be formed during this transition (see panel a in Fig. 4)

3.2. Thermal pulses after the AGB (late thermal pulses)

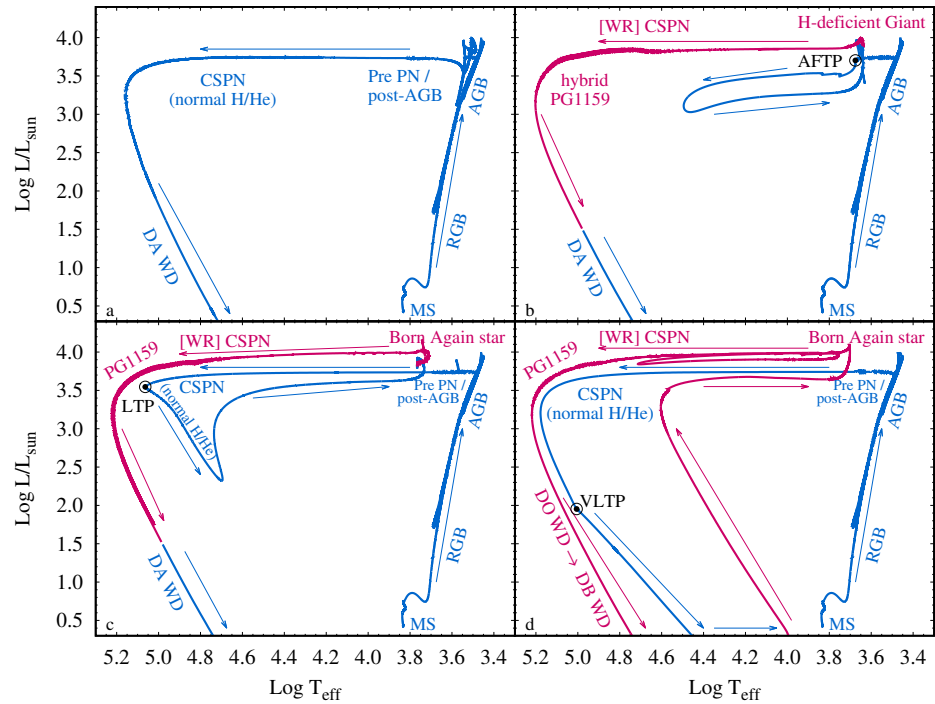


Figure 4. Evolution on the HR diagram of an initially $1.25M_{\odot}$ star from the main sequence (MS) to the final WD phases. Particular emphasis is done on the departure from the AGB into the post-AGB/pre-PN phases, and the formation of a PN and its central star. Arrows indicate the direction of the evolution. Blue line indicates the regions in the HR diagram where the model shows a H-rich surface composition, while magenta lines indicate a strong H-deficient surface composition. Panel a: canonical post-AGB evolution. Panel b: formation of a H-deficient CSPN after an AGB final thermal pulse (AFTP). Panel c: formation of a H-deficient CSPN after a late thermal pulse (LTP). Panel d: formation of a H-deficient CSPN after a very late thermal pulse (VLTP).

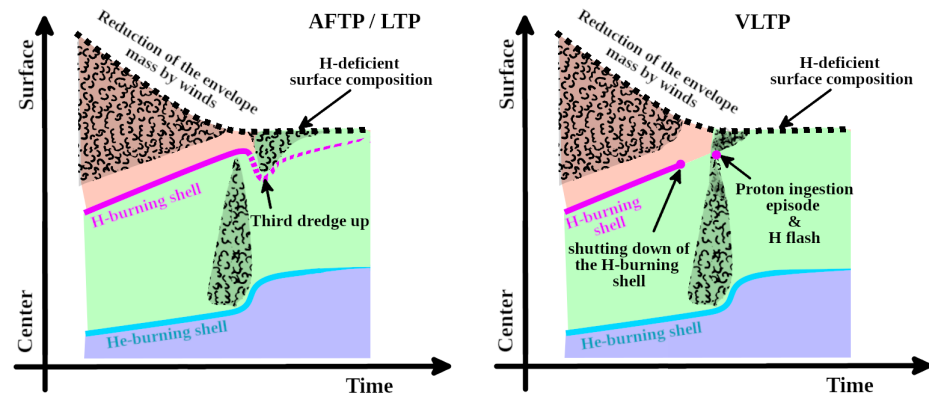


Figure 5. Schematic Kippenhahn diagrams of the internal structure of a post-AGB star that undergoes an AFTP/LTP (left) or a VLTP (right).

Of particular interest to us is the fact that the thermal pulses described in Section 3.1 can occur when most of the envelope of the star has been removed by the stellar winds, and the star is evolving towards the white dwarf phase [108] (see Fig. 4). These thermal pulses are then called late thermal pulses. In these cases, the sudden injection of energy by the thermal pulse pushes the star back into a giant configuration, giving rise to what have been called born again AGB stars [39] (see panels c and d in Fig. 4). For this reasons late thermal pulse scenarios are collectively mentioned as the born again scenario. Depending on the exact moment in the post-AGB evolution in which the late thermal pulse occurs, different outcomes are possible. And several of them can lead to the formation of a star with a H-deficient surface composition. Ref. [109] offers a useful classification of late thermal pulses into three categories: 1) AGB final thermal pulse (AFTP, panel b in Fig. 4) which occur just as the star is coming out of the AGB, and the H/He-envelope mass is about of $M_{\text{env}} \sim 10^{-2}\text{--}10^{-3}M_{\odot}$ ⁸; 2) late thermal pulse (LTP, panel c in Fig. 4) when the thermal pulse occurs during rapid evolution at constant luminosity, and the mass of the H/He envelope is $M_{\text{env}} \sim 10^{-4}M_{\odot}$; and 3) very late thermal pulses (VLTP, panel d in Fig. 4) when the thermal pulse occurs once the H-burning shell layer has decreased its intensity by more than an order of magnitude ($M_{\text{env}} \lesssim 10^{-4}M_{\odot}$), the luminosity of the star has fallen by more than 2 or 3 orders of magnitude, and the star is entering the WD phase. Each flavor of the thermal pulse leads to different chemical abundances in the photosphere of the CSPNe. Examples of the predictions of different models available in the literature are shown in Table 1.

If the dredging-up processes that bring material to the surface of the AGB star are active (the so-called third dredge up, 3DUP), the AFTP and LTP scenarios predict the formation of H deficient stars once the star returns to the giant branch and the outer convective zone deepens. As shown in Fig. 5 (left panel) if third dredge up is active, after the thermal pulse (either LTP or AFTP) convective motions in the envelope will penetrate into the He-, C- and O- rich intershell. However, contrary to what happens on the AGB, now the H-rich envelope has a very low mass, as most of it was removed by winds on the AGB. The mass of the H-rich envelope is now comparable (AFTP) or smaller (LTP) than the amount of mass dredged up from the intershell. This leads to a strong He, C and O enrichment of the envelope of the star that can be directly observed at the photosphere. Due to the difference in the mass of the remaining H-rich envelope, AFTP and LTP scenarios predict different final abundances for the star. While the LTP predicts final abundances of H of $X_H \lesssim 0.05$ (in mass fraction), AFTP predicts significantly higher abundances of $X_H \gtrsim 0.1$. In both cases the predicted final surface abundances are extremely enriched in He, C and O. It is worth emphasizing that the AFTP and LTP scenarios predict these abundances only if 3DUP is active. If this is not the case surface abundances remain unchanged and the result will be an CSPNe with an H/He ratio close to solar.

On the contrary the VLTP scenario (see panel d in Fig. 4) always predicts an extremely H-deficient surface composition. This is because, in a VLTP, H is violently burnt [110], instead of being just diluted. In a VLTP the thermal pulse happens once the H-burning shell has already died out and the star is already entering the WD phase (see right panel in Fig. 5). Due to this the entropy barrier that normally prevents the contact between the PDCZ and the H-rich envelope is strongly reduced [111], and the PDCZ is able to penetrate the H-rich envelope, dragging inwards the H-rich material into the hot He-burning regions. H is then violently burnt with ^{12}C , and later also with ^{13}C and ^{14}N , leading to a H-flash and a strong depletion of the H content of the star. A detailed description of these processes can be found in [56]. In addition to the formation of a strongly H-deficient surface composition, the VLTP might also lead to the formation of heavy elements through intermediate neutron capture process [112]. Since the early works [38,39,108] several

⁸ The envelope masses associated to each type of late thermal pulse given here are for $M_{\text{CSPN}} \simeq 0.6M_{\odot}$ central stars. More massive remnants will have less massive H/He envelopes at each phase. For a $M_{\text{CSPN}} \gtrsim 0.8M_{\odot}$ AFTPs will happen with envelopes of $M_{\text{env}} \sim 10^{-5}\text{--}10^{-4}M_{\odot}$, LTPs will have $M_{\text{env}} \sim 10^{-4}\text{--}10^{-5}M_{\odot}$ and VLTPs $M_{\text{env}} \lesssim 10^{-5}M_{\odot}$

authors have computed the formation of H-deficient CSs after a VLTP. In order to compute the simultaneous burning and mixing of the H-rich material into the He- and C-rich intershell it became a standard practice in 1D stellar evolution models to adopt a diffusive convective scheme [56,95,110,113–117]. The predicted abundances vary depending on the details of the evolutionary models but some generalities can be described. First and foremost it should be noted that the main composition of the resulting H-deficient star mostly reflects the previous He- and C- dominated composition of the intershell [110]. This composition varies with the number of thermal pulses and the initial mass of the star [118]. It is important to point out that the O abundance is strongly dependent on the assumptions about CBM at the bottom of the thermal pulse driven convective zone [113]. In order to reproduce the O-enriched observed in PG1159 and [WR] stars ($\sim 10\%$ to $\sim 15\%$ by mass fraction) mixing beyond the bottom of the pulse driven convective zone needs to be added and calibrated [113,118]. Table 1 shows surface abundances of different post-VLTP models once they become H-deficient. Fig. 1 shows post-VLTP evolutionary tracks and isochrones from [57,58]. When compared with H-rich central stars of similar mass (e.g. figure 8 in [118]) massive H-deficient CSPNe evolve slower, and stay brighter for a longer time, than their H-rich counterparts.

A different classification of late-helium flashes was proposed by [115]. In their classification, Type I models leave the AGB during the hydrogen-burning phase and continue like that until they reach the WD cooling stage and never become H-deficient. Type II models corresponds exactly to the VLTP classification described above, and always become H-deficient. Types III and IV models experience a helium shell flash after leaving the AGB, but do it while the H-burning shell is active, so that H is not burnt. The difference between types III and IV models is based on the effective temperature of the star when the helium shell flash occurs ($T_{\text{eff}} > 30000\text{K}$, Type III, and $T_{\text{eff}} < 30000\text{K}$, Type IV). Consequently, all Type III for models correspond to LTP cases, while Type IV corresponds to LTP and AFTP cases. Finally⁹, Type V models leave the AGB during a helium shell flash and type VI models leave the AGB during quiescent helium burning. Some type V and VI models become slightly H-deficient. In addition to these types, [119] added a transition type II/III for those models that reach peak helium-burning luminosity when $T_{\text{eff}} > 100000\text{K}$ and the H-burning shell is decreasing its luminosity but its still quite active. In his work [119] the author reports that in their computations (in which no CBM is applied to the PDCZ) type II/III models consume about half the H.

⁹ Lawlor [115] also defines four more type for those high metallicity sequences that, in their sequences, evolve away from the AGB before reaching the phase of thermal pulses.

Table 1. Typical surface abundances (by mass fractions) of post-VLTP, post-LTP and post-AFTP evolutionary models that lead to the formation of H-deficient central stars (during the PG1159 and [WR] stages). M_i and M_f indicate the initial (zero age main sequence) and final (WD stage) masses of each evolutionary sequence. Note that models with $Z_0 = 0.02$ were computed with slightly different assumptions for CBM than $Z_0 = 0.01$ and $Z_0 = 0.001$ models.

M_f [M_\odot]	flavor	H	^4He	^{12}C	^{13}C	^{14}N	^{16}O	^{20}Ne	^{22}Ne	M_i [M_\odot]	Z_0	Ref.
0.530	VLTP	9×10^{-3}	0.33	0.39	0.051	0.0192	0.17	1.6×10^{-3}	0.0194	1.0	0.02	[57]
0.542	VLTP	6.9×10^{-3}	0.28	0.41	0.051	0.0178	0.213	1.6×10^{-3}	0.0192	1.0	0.02	[57]
0.561	VLTP	1×10^{-4}	0.33	0.32	0.053	0.0289	0.232	1.6×10^{-3}	0.0275	1.8	0.02	[58]
0.564	VLTP	1.1×10^{-3}	0.39	0.27	0.048	0.0265	0.217	1.7×10^{-3}	0.0380	2.2	0.02	[57]
0.584	VLTP	~ 0	0.40	0.31	0.055	0.0362	0.170	1.6×10^{-3}	0.0295	2.5	0.02	[57]
0.609	VLTP	~ 0	0.50	0.35	3.1×10^{-3}	2.1×10^{-3}	0.103	1.6×10^{-3}	0.0355	3.05	0.02	[57]
0.664	VLTP	~ 0	0.47	0.33	0.019	0.0128	0.126	1.9×10^{-3}	0.0328	3.5	0.02	[57]
0.741	VLTP	~ 0	0.48	0.34	7.1×10^{-3}	2.5×10^{-5}	0.139	0.0026	0.027	3.75	0.02	[58]
0.870	VLTP	~ 0	0.54	0.30	9.9×10^{-3}	8.3×10^{-3}	0.0938	0.0061	0.0171	5.5	0.02	[57]
0.480	VLTP	0.030	0.52	0.30	0.041	0.016	0.086	9×10^{-5}	1×10^{-3}	0.8	0.001	[95]
0.537	VLTP	5×10^{-3}	0.48	0.29	0.069	0.065	0.091	9×10^{-5}	9×10^{-4}	0.9	0.001	[95]
0.535	VLTP	5×10^{-5}	0.40	0.34	0.074	0.056	0.116	9×10^{-4}	0.01	1.0	0.01	[95]
0.552	VLTP	5×10^{-3}	0.38	0.37	0.059	0.028	0.145	9×10^{-4}	0.01	1.1	0.01	[95]
0.567	VLTP	5×10^{-6}	0.41	0.33	0.067	0.047	0.133	9×10^{-4}	0.01	1.25	0.01	[95],Fig. 4
0.565	LTP	0.049	0.33	0.36	4.8×10^{-7}	7.2×10^{-5}	0.21	1.7×10^{-3}	0.038	2.2	0.02	[120]
0.589	LTP	0.040	0.31	0.40	0.0138	1.4×10^{-3}	0.20	1.7×10^{-3}	0.020	2.7	0.02	[120,121]
0.567	LTP	9×10^{-3}	0.42	0.43	5.5×10^{-7}	1.5×10^{-4}	0.12	9×10^{-4}	0.01	1.25	0.01	Fig. 4
0.566	AFTP	0.137	0.39	0.36	6×10^{-4}	6×10^{-4}	0.104	8.5×10^{-3}		1.25	0.01	[53],Fig. 4
0.550	AFTP	0.197	0.45	0.30	1×10^{-4}	1×10^{-4}	0.056	7.8×10^{-4}		1.0	0.001	[53]
0.594	AFTP	0.219	0.45	0.26	7×10^{-4}	7×10^{-4}	0.055	0.021		1.5	0.001	[53]

Lawlor [119,122] presented a detailed grid of stellar evolution models of LTP events. Their models cover a wide metallicity range ($Z = 0.0015\text{--}0.03$) but are only focused in LTP events in low-mass progenitors ($0.9M_{\odot} < M_i < 2M_{\odot}$). As these simulations do not include CBM most models never become H-deficient. Only a few of their TP models (their "type II/III" models), those that erupt at the highest temperatures (very close to the boundary with VLTP cases), and with the smallest radii become modestly enriched in He, C, N, and O. This may be relevant for CSPNe that are only modestly H deficient. On the contrary, models that include CBM, and favor the development of 3DUP [121,123,124] lead to much stronger H deficiencies ($H \sim 0.05$ by mass fraction). H deficiency is attained after the return to the AGB, when third dredge up develops in the post-LTP giant [123]. In these cases He, C and O abundances are very similar to those predicted by the VLTP case, as the model is displaying its previous intershell abundances at the photosphere (see Figs. 3 and 5). The main difference is in the isotopic $^{13}\text{C}/^{12}\text{C}$ ratio, as VLTPs lead to a strong production of ^{13}C and in many cases also ^{14}N . Table 1 shows surface abundances for some post-LTP models that became H-deficient.

The number of AFTP models in the literature resulting in H-deficient surface compositions is very limited [53,115,125]. For those models that undergo third dredge up [53,125] the final surface composition of H is between $X_H \sim 0.1$ and $X_H \sim X_H^{\odot}$ depending on how massive the remaining H-rich envelope is at the moment of the helium flash. As in LTP cases, the final O abundances are strongly dependent of the assumed CBM during the previous AGB evolution (see Table 1).

Besides 1D stellar evolution simulations, in the last two decades 3D hydrodynamical simulations of the H entrainment in the He-shell flash convective zone during a VLTP event became possible [112,126,127]. These simulations show a very rich complexity of hydrodynamic processes that cannot be captured by 1D stellar simulations of the event. Unfortunately, 3D hydrodynamical simulations are very demanding. Current simulations of the convective reactive ingestion of protons into the He-burning shell during a VLTP can only be performed for a very short physical time, a snapshot in the development of the VLTP. Simulations by Herwig et al. [112,126] correspond to physical times of about a day in the life of the star. Consequently, the development of the violent H-flash cannot be followed and simulations need to be started from an artificial background model where the H-flash develops as soon as possible. In spite of this, 3D-hydrodynamical simulations are very informative, inspired by 3D hydrodynamical simulations it was suggested [112] that the splitting of the convective zones created by the violent H-burning during H-entrainment could be delayed, leading to observable signatures in the nucleosynthesis by intermediate neutron capture processes¹⁰. More interestingly, the simulations of the H ingestion flash performed by [112,126] found the formation of global non-spherical oscillations that are sustained by individual ignition events of H-rich fluid pockets. This result is particularly interesting in view of the plethora of non-spherically symmetric features found around H-deficient CSPNe [89] (see Section 2.3). Moreover, 3D hydro simulations have been used to inform simplified 1D models of convective mixing. For example, [129] 3D-hydro simulations were used to construct a 1D advective two-stream model for the computation of detailed nucleosynthesis.

The final evolutionary state of stars undergoing an AFTP, LTP or VLTP deserves some comment. It is a well known fact that once stars enter the WD cooling track, winds fade and gravitational settling takes over, leading to the formation of the observed almost pure (H or He) atmospheres of WDs [see 130, for a detailed review of WD evolution]. Even tiny amounts of diluted H ($M_H \simeq 10^{-14}M_{\odot}$) can lead to the formation of a WD with pure H atmosphere (DA WD) [131]. In the AFTP and LTP cases where a H-deficient CSPNe was formed after 3DUP, the H diluted into the deeper parts of the envelope is later burned as the star contracts again to the WD cooling track leading to a decrease in the H content of the

¹⁰ Intermediate neutron capture processes happen at neutron densities intermediate to those of the classical slow ($N_n \sim 10^7\text{--}10^{11} \text{ cm}^{-3}$) and rapid neutron capture processes ($N_n \sim 10^{20} \text{ cm}^{-3}$) [128].

WD. Once winds stop and gravitational settling takes over both post-LTP and post-AFTP stars are expected to form DA WDs. In the case of post-LTP stars DA WD with very thin H envelopes are expected, with H-contents as low as $M_H \simeq 10^{-6}$ – $10^{-7} M_\odot$ [116,121] (see Fig. 4). The final fate of post-VLTP remnants is less understood. It has long been argued that post-VLTP stars will form H-deficient WDs (DO, DB, DC and DQ WDs, see Fig. 4)[124]. However the complete destruction of H seems to be very difficult in stellar models, either through burning or winds on the [WR] stage. For the case of post-VLTP stars with masses $M_f \simeq 0.6 M_\odot$, [132] obtained DA WDs with H contents as low as $10^{-11} M_\odot$. Better models are needed to clarify whether post-VLTP stars end up as DA or non-DA WDs.

3.3. Advantages and successes of the born again scenario

Although the return stage to the AGB after the thermal pulse is extremely fast in evolutionary terms, some stars have been identified going through these very fast stages. Four CSPNe have been measured to change their surface properties (T_{eff} , L_* , g and even composition) in the short timescale of a few years or decades corresponding to late thermal pulses (FG Sge, V605 Aql, V4334 Sgr, and Hen 3-1357, see Appendix A). Of these stars, V605 Aql and V4334 Sgr have been identified as VLTP cases, while FG Sge and Hen 3-1357 seem to be LTP cases. These born again stars not only offer a confirmation that late thermal pulses actually occur in nature, but also demonstrate the link between AGB stars and CSPNe. Moreover, they allow testing different particularities of stellar evolution models and their nucleosynthesis [133] (see Appendix A). V4334 Sgr, FG Sge, and also V605 Aql demonstrate that the born again scenario actually leads to the formation of H-deficient CSPNe, and also, that it can lead to the formation of [WO] CSPNe [134–137]. Moreover, the born again scenario offers a natural qualitative explanation for the similar abundances found in [WC], [WO], and PG1159 spectral types, and also to the luminosity and photospheric temperatures and gravities of these stars, linking them to a natural evolutionary post-AGB sequence, see lower panel of Fig. 4.

Maybe the most appealing characteristic of the born again scenario is that its occurrence is statistically unavoidable [38,39,108]. Given that the occurrence or not of the born again scenario (and its flavors, VLTP, LTP, AFTP) is only a consequence of the relation between the timing of thermal pulses and the timing of the removal of the envelope of the AGB star [106], and these two clocks run independent from each other, for a given initial mass and metallicity it is expected that a sizable fraction of all single stars will undergo a born again event. This fraction is expected to be somewhere around $\sim 20\%$ [39]. In the absence of any theoretical argument suggesting that the departure from the AGB always happens at the right phase to avoid a late helium flash, one should come to terms with the idea that late thermal pulses happen in a sizeable minority of single post-AGB stars, and form H-deficient CSPNe through this channel. Current estimations of the multiplicity of low- and intermediate-mass stars [138] indicate that the close binary fraction ($a < 10\text{au}$) is of about $\sim 20\%$ for stars with initial masses of $M_i \simeq 1 M_\odot$ and rises to $\sim 55\%$ for stars with $M_i \simeq 6 M_\odot$. This means that between 80% and 45% of all intermediate and low mass stars evolve mostly unperturbed by possible companions. The large number of stars evolving in isolation or in wide binaries, together with the sizeable fraction of stars for which departure from the AGB will result in a born again event, is a compelling argument in favor of the idea that many H-deficient CSPNe and post-AGB stars have a born again origin.

Besides its ubiquity, one of the most successful features of the born again scenario is its ability to reproduce the rare He, C, and O atmospheres of both [WC], [WO] and PG1159 stars [109,113]. Qualitatively, it is very unlikely to have layers in the interior of a star where He, C, and O can coexist. The existence of He, C and O in the surface of [WC], [WO] and PG1159 stars links them almost exclusively to the intershell of AGB stars. A possible exception to this might be the outcome of the merger of two low-mass CO-core WDs or the merger of a low-mass CO-core WD and a more massive He-core WD [139]. However, in these cases the formation of a PNe with normal H/He composition would be impossible to explain. Conversely, the born again scenario naturally explains the presence of a PNe

with a normal H/He composition. Additionally the late thermal pulse scenario could help understand how bipolar nebulae could form around isolated stars [89,126,140]. The late thermal pulse scenario is a key piece of the current understanding about the formation of around of 20% of the CSPNe, which show H deficiency [31,141].

A final argument in favor of the late flasher scenarios (AFTP, LTP, VLTP) can be made from their predictions for the final WD stage. The existence of single WDs with extremely thin H envelopes (of the order of $M_H \simeq 10^{-14} M_\odot$) has been invoked to explain the spectral evolution that WDs seem to experience as they evolve [130,142,143]. More specifically the recent study by [142] indicates that 60% of WDs must have a H contents larger than $M_H = 10^{-10} M_\odot$, another 25% have H contents in the range $M_H = 10^{-10} M_\odot - 10^{-14} M_\odot$, and 15% have H contents lower than $M_H = 10^{-14} M_\odot$. The existence of DA WDs with very thin H envelopes has also been inferred from asteroseismological studies of variable DA WDs [144,145]. Such low-H content WDs cannot be explained by canonical single stellar evolution (panel a, Fig. 4) which predicts that WDs should be formed with a total H content of $M_H \simeq 10^{-3} - 10^{-5} M_\odot$, depending on the stellar mass and metallicity of the progenitor [146]. As discussed in Section 3.2 these single DA WDs with thin H contents are naturally explained by LTP and VLTP scenarios [132].

3.4. Shortcomings of the born again Scenario

Despite its many successes, the born again scenario faces serious challenges as it is unable to explain many observed features in H-deficient CSPNe and their PNe. In fact, none of the bona fide late helium flashers discussed in Appendix A evolved exactly like models predicted. For example, while the T_{eff} evolution of Hen 3-1357 is well reproduced by an LTP in a low-mass remnant ($0.53 < M_{\text{CSPN}}/M_\odot < 0.56$, [147]) the surface gravity of Hen 3-1357 is systematically higher than that predicted by LTP models [122,147]. Similarly, while the pre-outburst and post-outburst evolution of V605 Aql and V4334 Sgr can be reproduced by standard VLTP models of different masses [58,148] no single model is able to simultaneously reproduce all these observables. Moreover, as mentioned before, both the 1921 spectra of V605 Aql and the 1996 spectra of V4334 Sgr show much higher He abundances and very little C in comparison with the intershell abundances of AGB stars and VLTP models.

With no hope of being exhaustive in this section we will mention some of the shortcomings and failures of born again models. In this connection we can mention that the properties of the H-deficient material ejected around some H-deficient CSPNe are at odds with our current understanding of the the born again scenario. The abundances on the H-deficient knots around Abell 30 [99] and Abell 58 [97] were found to have $C/O < 1$ and the presence of substantial quantities of neon (Ne) ($\sim 34\%$ and $\sim 13\%$ respectively¹¹), respectively at variance with the predictions of the born again scenario. It should be noted, however, that according to [149] if the carbon trapped into dust grains is taken into account then the C/O ratio of the H-deficient ejecta is larger than 1, and in agreement with the born again scenario. Another problem for the born again scenario are the He/C/O abundances of the H-deficient knots of Abell 58 and Abell 30 which are not in agreement with the current abundances of their CSs which show typical PG1159 He/C/O abundances (and show [WCE]-PG1159 spectral types). It should be noted however that, if shocks are indeed the dominant excitation mechanism, the current nebular abundance estimates [97,150] should be revisited. Moreover studies of Ne and O abundances in the H-deficient ejecta in Abell 30 [99], Abell 58 [97] and Abell 78 [151] found a very high Ne/O ratios not in agreement with the predictions of the born again scenarios. In addition to the abundance inconsistency, there is a clear discrepancy between the geometries of the outer and inner nebular regions of both Abell 30 and Abell 78. The outer H-rich shells are ellipsoidal and expand at $\sim 40 \text{ km s}^{-1}$, while the H-deficient knots detected have much larger velocities of up to 200 km s^{-1} .

¹¹ In the case of Abell 30 this is true only for one of the knots analyzed as the Ne abundance is not the same for all of them.

s^{-1} . The central parts in Abell 30 and Abell 78 were imaged by the Hubble Space Telescope and revealed structures distributed on an equatorial plane and polar features [91,152]. Both the strong axisymmetrical shape of the inner regions and their high Ne abundances have been used to link these objects to possible binary evolution channels (see Section 4.1).

Another feature that hints that the born again scenario cannot be the only formation scenario for H-deficient CSs is the detection of close binary stars with H-deficient compositions. Jacoby et al [102] report the presence of light curve brightness variations having a period of $P_{\text{orb}} = 1.060$ d in Abell 30, hinting at the possibility of a close binary CS. A similar discovery was reported by [153] who found a significant periodic variability hinting at a close binary ($P_{\text{orb}} = 4.04$ d) near the [WO] CS of NGC 5189. The presence of a close binary companion within the born again scenario is not easy to reconcile. For that situation to happen it would be necessary that the VLTP happens immediately after the common envelope event, as otherwise the H-burning shell would still be active and not VLTP would occur. Yet, if a VLTP were to occur in a close binary system the expansion following the VLTP would lead to the engulfing of the companion and the destruction of the close binary. Similarly, for the same reasons it is very difficult to imagine a born again origin for the only known PG1159 star in a close binary [154,155]. These observations indicate that there might be a binary evolution channel able to produce the typical [WR]/PG1159 surface compositions. We will see in the next sections that this suggestion is not devoid of problems. It is worth noting that the case of NGC 246 does not pose a problem for the born again scenario as the members of the triple system are relatively distant [17].

A very well known problem for the born again scenario arises from the lack of intermediate spectral types in Wolf-Rayet central stars ([WC 5-7]). This can be appreciated in Fig 1 as a dearth of stars at about $T_{\text{eff}} \simeq 50000\text{K}$. Due to the expected evolution on the HR diagram after the return to the AGB (see Fig. 4), one would expect that the second contraction of the, now H-deficient, CSPNe would follow the spectral sequence [WCL]→[WCE]→PG1159, and then due to the action of gravitational settling into DA WD or DO WD stars¹² depending on the amount of H remaining in the envelope [116,121,124,156]). Consequently, under the born again scenario the absence of intermediate spectral types in [WR]-CSPNe is difficult to explain. Whether this is feature is real or a consequence of the different spectral lines adopted for the determination of the surface properties of early and late [WR] stars is not known.

Moreover it has been argued that there is a discrepancy between the abundances of C and He of early and late [WC] types. While [WCL] were determined to have similar He and C mass fractions (He/C/O 0.4/0.5/0.1, [34–36,157] similar to those observed in PG1159 stars, the earlier [WCE] were determined to have twice as much He than C by mass fraction [WCE] He/C/O 0.6/0.3/0.1 [55,158,159]. A similar situation happened for transition types [WC]-PG1159 (Abell 30 & Abell 78) He 0.65, C=0.20...0.30, N=0.015, O=0.15. However this discrepancy has been questioned by some authors, finding similar C and He abundances for [WCE] and [WCL] (He/C/O 0.45/0.45/0.1 [160,161]. To date, [WCL] have not been reanalyzed systematically with improved line-blanketed stellar atmosphere models. The latter determinations of abundances in [WR] stars with modern atmosphere models seem to suggest that both groups might have similar abundances (see Table 2).

¹² DA WDs show almost pure H atmospheres with, at most, traces of other elements (DAZ spectral type) and represent the vast majority of WDs. WDs with He dominated atmospheres are a minority and sometimes known as non-DA WDs. Non-DA WDs are divided into several subclasses: DO WDs ($45000\text{ K} < T_{\text{eff}} < 200000\text{ K}$), DB WDs ($11000\text{ K} < T_{\text{eff}} < 30000\text{ K}$), and DC, DQ, and DZ types ($T_{\text{eff}} < 11000\text{ K}$) depending which trace elements are visible in their spectra. See [130] for a detailed review.

Table 2. Recent determinations of surface abundances in [WCL], [WCE], and [WO] CSPNe.

Name	Spectral type	[H/He/C/N/O/Ne] (mass fractions)	Reference
HuBi 1	[WC10]	0.01...0.05/0.33/0.5/0.01/0.1/0.04	[95]
SwSt 1	[WC9/10]	0 /0.42/0.50/0.05/0.03/0.02	[162]
NGC 40	[WC8]	0 /0.57/0.4/1.e-3/0.03/<0.03	[163]
NGC 2371	[WO1]	0.71/0.20/0.001/0.06/0.03	[164]
NGC 6905	[WO2]	<0.05/0.55/0.35/7e-5/0.08/0.02	[165]
NGC 1501	[WO4]	-/0.6/0.3/0.15/-/-	[166]
Abell 30	[WCE]-PG 1159	-/0.63 /0.20 / 0.15 / 0.015/-	[167]
Abell 78	[WCE]-PG 1159	-/0.55 /0.30 / 0.10 / 0.015 / 0.04	[168]

Another problem for the born again scenario comes from different estimations of the spatial distribution of normal CSPNe, PG1159, and [WR] stars. In their work, Weidmann et al. [31,141] found that the galactic latitude distribution of H-rich and H-deficient CSPNe is different, with H-deficient CSPNe closer to the galactic plane. That would be an indication that the progenitors masses and ages of both populations are different, with the progenitors of H-deficient stars more massive and younger than their H-rich counterparts. While this is not in strong contradiction with the born again scenario it would require the frequency of late thermal pulses to increase with mass, while the opposite is hinted by models, where the shortening of post-AGB timescales with mass [118] happens much faster than the shortening of the interpulse cycle with mass, making late flashes less probable. Moreover, a more serious problem has been suggested by a new catalog of distances to PNe based on Gaia parallaxes [169]. By deriving distances in a homogeneous way for 2211 objects the authors find that [WR] CSPNe are closer to the Galactic plane than H-rich CSPNe. Most importantly, the authors find that [WR] CSPNe are closer to the galactic plane than other H-deficient CSPNe (such as PG 1159, O(He) and DO WDs), with the latter having similar distribution to H-rich CSPNe. If this is confirmed it would suggest that [WR] CSPNe have more massive progenitors than PG1159 CSPNe (see also [170], making the evolutionary connection impossible for most of these stars. This later result is at variance with the earlier work of [171] who analysed the observational data for PNe with H-deficient CSPNe and concluded that it suggested the evolutionary sequence the general evolutionary sequence [WCL]→[WCE]→PG 1159. Noteworthy, this work also concluded that the observed parameters of PNe were not consistent with the theoretical models of the born again scenario available at that time [171]. A reanalysis in light of updated models of the born again scenario is necessary.

Finally, it is clear that the born again scenario is unable to explain the properties of the He-rich sequence of CSPNe (O(He), DO, and some [WN], see Table 3). Note that while it is expected that DO stars are formed from PG1159 stars, the timescales for gravitational settling turning a PG1159 star into a pure DO WD are much longer than any expected lifetime for a PNe [116]. Consequently, those DO that are CSPNe cannot descend from PG1159 CSs. While objects such as PB 8 and Hen 2-108 have H/He abundances not far from those of H-PG1159 stars and might be evolutionarily connected (see Table 3, although C abundances greatly differ) the situation is very different for the "pure" [WN] stars (IC 4663 and Abell 48). Both IC 4663 and Abell 48 show extreme He abundances, similar to those of the O(He) and DO CSPNe, but very different from those predicted by all flavors of the born again scenario. These abundances are very similar to those observed in RCrB stars [172], and consequently have been connected to possible merger episodes (see Section 4).

Table 3. Recent abundance determinations [WN], O(He), DO, and Hybrid-PG1159 (H-PG1159) CSPNe.

Name	Spectral type	[H/He/C/N/O/Ne] (mass fractions)	Reference
IC 4663	[WN 3]	<0.02/0.95/<0.001/0.008/0.0005/0.002	[43]
Abell 48	[WN 5]	0.1/0.85/0.03/0.05/<0.006/-	[49]
PB 8	[WN 6/WC 7]	0.4/0.55/0.01/0.01/0.01/-	[163]
Hen 1-108	[Of/WN 8]	0.50/0.48/ 7×10^{-5} / 1.4×10^{-5} / 5.7×10^{-5}	[173]
K 1-27	O(He)	0.046/0.933 / 5.6×10^{-4} /0.0132/ 5×10^{-5} /0.005	[47]
LoTr 4	O(He)	0.12/0.871/< 7.2×10^{-4} /0.0079/< 1.9×10^{-4} /<0.001	[47]
Abell 43	H-PG1159	0.25/0.46/0.27/0.0026/0.0044/0.012	[53]
NGC 7094	H-PG1159	0.15/0.52 / 0.31 / 3×10^{-4} / 0.0033 / 0.0019	[53]
KPD 0005+5106	DO	<0.025/0.977/0.01/0.0025/0.004/0.01	[174]

4. PNe progenitors and binary stellar evolution

It is a well known fact that binarity in low- and intermediate-mass stars is not as ubiquitous as in massive stars [138,175]. However, the multiplicity fraction changes dramatically in the range of masses expected for the progenitor stars of PNe. For example, for KGF main sequence stars (initial masses $0.75M_{\odot} < M_i < 1.5M_{\odot}$) the fraction of stars in multiple systems is reported to be between 42% and 50% [138], but it rises to about 70% for A stars ($\sim 2M_{\odot}$), and then to $\sim 80\%$ for late B stars ($3M_{\odot} < M_i < 5M_{\odot}$), and to $\sim 90\%$ for early B stars ($5M_{\odot} < M_i < 8M_{\odot}$). Nevertheless, while wide binaries might affect the shape of the PNe they are unable to alter the evolution and lead to true binary evolution channels. For example, FGK main sequence stars follow a broad lognormal separation distribution peaking near $a = 40$ au [175,176], so most low-mass stars will follow single star evolution paths, regardless of the existence of a companion¹³. This said, the close binary fraction among low- and intermediate-mass stars is not negligible. In fact the close binary fraction ($a < 10$ au) is between 20% and 25% for FGK main sequence stars, rises to $\sim 37\%$ for A-type stars, and then to $\sim 46\%$ and $\sim 55\%$ for late- and early-type B stars respectively [138,175,176].

In the following paragraph we will very briefly describe some of the intricacies of binary stellar evolution, the reader interested in the many physical processes and details of binary stellar evolution is referred to specialized books and reviews on the topic [e.g. 177–180]. One of the main mechanisms of interaction in a binary system is the transfer of mass (and angular momentum) between the components of the system. The most important modes of mass transfer are: Bondi–Hoyle–Lyttleton (BHL) wind accretion [181], the wind accretion through Roche lobe overflow (WRLOF) [182], stable mass transfer by Roche Lobe Overflow (RLOF) [183], and unstable mass transfer with the consequent formation of a common envelope (CE) [184]. In addition to these processes interaction through tides and magnetic fields can also play a role in the orbital evolution of the system [185–187]. All these phenomena have as a consequence the transfer and/or loss of angular momentum between the components and change the orbital parameters of the system. The two dominant parameters in defining the evolution of the system are the distance (a) and the mass ratio $q = M_2/M_1$ between the components. The mass transfer can occur on dynamic, thermal, or nuclear time scales, depending on the mass ratio and the response of the radius of the donor star to mass loss. The type of mass transfer that occurs in a particular system depends primarily on whether the stellar envelope of the donor is convective or not (which determines how the star radius reacts to mass loss), and how the ratio of masses between both stars is (which determines how the size of the Roche lobes changes as mass is transferred/lost from the system).

When the mass transfer occurs on a very short a time scale the envelope of the accreting star is pushed away from the so-called thermal equilibrium (steady state). Because of this it

¹³ The evolution might involve, however, the interaction with substellar companions.

expands and might form a common envelope around both stars. A common envelope will lead to rapid decay of the orbit, due to drag forces and the transfer of energy and angular momentum to the common envelope [184]. If the envelope is ejected the result it will be a close binary surrounded by the ejected material. If, in addition, the temperature evolution of the remnant, and the gas dispersion times, are favorable this will lead to the formation of a planetary nebula with a close binary inside.

The critical mass ratio for mass transfer to be unstable is not well determined. Recent studies indicate that, for conservative mass transfer, mass transfer would only be unstable for values of $q > 1.5$ – 2 [188], greater than the threshold value of $q \sim 0.8$ that emerged from more idealized studies [189]. When the mass transfer is stable the system widens or shrinks depending on whether the system loses some of its mass and angular momentum during mass transfer [178]. In relation to the formation of planetary nebulae, [190] studied the orbital evolution of binary systems where the donor is an AGB star. There, using simulations of stars of $1M_{\odot}$ with $q = 2$ and $q = 10$ (i.e. companions of 0.5 and $0.1 M_{\odot}$), and initial separations between 3 and 10 AU (periods from 5 to 26 years), found that systems with a separation greater than ~ 6 AU (periods of ~ 12 years or ~ 4380 days) end in more distant orbits as a consequence of BHL mass transfer while those systems with shorter distances end up in tighter orbits as a consequence of WRLOF mass transfer. So, systems at initial distances smaller than 6 AU would end up approaching each other as a consequence of the WRLOF, and could later evolve through RLOF and CE stages depending on the initial distance.

An additional comment regarding the impact of binaries on the formation of PNe refers to the time scales corresponding to contraction to the WD stage. Ref. [191] showed that models of stars undergoing rapid mass loss (with envelopes far from the thermal equilibrium) evolve much faster than the classical models where the stellar envelope is lost by stationary winds on time scales of thousands of years.

4.1. Proposed evolutionary channels for H-deficient CSPNe

The appeal of binary channels for the formation of H-deficient CSs is based on two very different circumstances. On the one hand binarity opens a large parameter space for the initial configuration of the system that might help to explain the diversity of CSPNe and PNe properties. This is in line with the studies of Abell 30 [102] and NGC 5189 [153] which suggest that both PN might harbor a close binary CSs. Moreover, the high ADFs observed in both Abell 30 and Abell 58 [97–99], together with the clear connection between strong ADFs and binarity [100] make binarity an appealing possibility. On the other hand, the lack of a quantitative understanding of unstable mass transfer and common envelope events [178,179,192,193] allows for broader speculation than single star evolution models. In this section we will only discuss some scenarios proposed in the literature for the formation of CSPNe with no hope of being exhaustive. The reader interested in the relevance and variety of binary formation channels of both CSPNe and PN is referred to specialized reviews and books [11,12,193,194].

One of the most appealing binary scenarios for the formation of H-deficient CSs is the merger of (low-mass) He-core WD with a more massive CO-core WD. It has been long shown that CO-core WD + He-core WD merger can explain the formation of the vast majority of RCrB stars [172,195–197]. RCrB stars have typical abundances of $X_{\text{H}} < 0.05$, $X_{\text{He}} \sim 0.98$ and traces of C, N, O below 1% by mass fraction [198,199]. These abundances are in qualitative agreement with what is expected from CO-core + He-core WD mergers, where the less massive He-core WD (composed of almost pure He and traces of N) is tidally disrupted and poured on top of the CO-core WD. The ignition of He in a series of shell flashes in the He-mantle is able to produce significant quantities of C and O while the star expands to its giant (RCrB stage) [196]. Due to the obvious abundance similarities between the abundances of RCrB stars and those of O(He) and some [WN] CSPNe (IC 4663 and Abell 48, see Table 3) it seems natural to link them evolutionarily. Moreover stellar structure models of RCrB stars predict that these objects will finally contract at

constant luminosity crossing the CSPNe region of the HR diagram, before finally becoming WDs [196,200,201]. Thus abundances of the CSPNe and post-merger evolutionary tracks, suggest the connection Merger \rightarrow RCrB \rightarrow EHe \rightarrow [WN] \rightarrow O(He) \rightarrow DO. The main shortcoming of this scenario is that the PNe surrounding all these He-dominated stars show normal H dominated compositions [43,50,202–206]. A relatively natural alternative would be to suggest that the merger takes place inside a common envelope which, once ejected, forms the PNe. Under this scenario one would expect the PN to be much more massive than normal PNe and strongly axisymmetrical, which does not seem to be the case [202,203].

A similar reasoning can be applied to the low-mass CO-core WD + He-core WD merger (or double low-mass CO-core WD merger) channel proposed in [139]. While it can explain the abundances observed both in PG1159 and [WR] CSs the existence of a normal (H-rich) PN around the merger product could only be explained if the merger happens during a common envelope event. As in the previous case one would expect the PN to be much more massive than normal PNe and strongly axisymmetrical.

Other binary scenarios have been proposed in the literature specifically tailored to explain certain properties of H-deficient CSPNe [207]. In this connection we can mention the engulfment/merger scenarios aimed at explaining the so-called double-dust chemistry of PNe¹⁴ and the H-deficiency of the CSPNe [208]. The authors proposed that, as the star reaches the AGB it engulfs a companion, which spirals in within the AGB envelope, leading to an increase in the AGB mass-loss rate. Then, the entire envelope is expelled as O-rich gas, and C-enhancement in the inner layers is induced by shear mixing caused by the engulfment of the companion. It is then assumed that the enhancement of mass loss also leads to the formation of a H-deficient central star. This scenario seems unlikely for several reasons. Besides the obvious speculative nature that prevents quantitative comparison, it has some problems even at the qualitative level. Most importantly, as most of the envelope would be ejected at a single event, we should expect most of the mass to be located close to the star, and a very massive PNe around the star. As mentioned before, those old nebula around H-deficient ejecta do not agree with these characteristics. It should be noted, however, that some fraction of the mass of the outer nebula could be in neutral form and hence missed from emission line studies. In addition to the low mass of the PNe, PNe around H-deficient stars are not particularly axisymmetrical. Moreover, the innermost region of the envelope, where the H-burning layer is located, and also the He-buffer below it are very tightly bound to the core of the AGB star and should be very difficult to be ejected during the merger process. In addition mixing might also be very difficult due to the presence of a strong entropy barrier between the envelope and the core [111]. Ejection of any remaining H-envelope through winds is also highly unlikely [132].

Another of the scenarios mentioned in the literature concerns the so-called “two-common envelope scenario” [207]. In this scenario it is assumed that a final thermal pulse might happen to one of the components of an already existing close binary system (after a previous, first, common envelope event). In such a scenario, the final thermal pulse would trigger a second common envelope event which should lead to the merger of the two components. It is speculated then, that the companion material would provide the H-rich gas that, together with C-rich wind of the newly formed [WCL] star, would lead to the formation of PAHs. Again, besides the speculative nature of the scenario, there are some key points that might even be problematic on a qualitative level. First, and foremost, it is not easy to envisage a situation in which a VLTP might happen after a first common envelope. For a final thermal pulse to happen the He-rich intershell needs to grow to a critical value, this happens due to the CNO fusion at the H-burning shell. In single stars, VLTPs happen when the AGB envelope is reduced, in thermal equilibrium, beyond a critical value through the action of winds [118]. As the star contracts towards the WD cooling track H-burning shell continues burning H and increasing the mass of the He-rich intershell [104]. This

¹⁴ The presence in the PNe of C-rich dust located inside a shell of O-rich dust (silicates).

would not be the case after the first common envelope event that forms the initial close binary. The fast removal of the envelope would lead the envelope away from thermal equilibrium [191] allowing (albeit not forcing) the removal of the envelope well beyond the aforementioned critical value. After the fast ejection of the envelope the remaining envelope is either above or below the critical envelope value. If it is well below, then the remaining H-rich envelope will be very likely too thin to allow the He-rich intershell to grow to a critical value and produce a VLTP, unless the situation is extremely finely tuned. If it is well above, then the star will still have a giant configuration and the companion has either been engulfed into the envelope of the primary, and merged, or it is still in a relatively wide orbit ($a \gtrsim 1\text{AU}$). In both cases the star will continue evolving as a single star. To the best of our understanding the only viable possibility for this scenario to happen is that the first common envelope event leads to the ejection of most of the envelope of the AGB star but not all, close to the critical envelope mass needed for the star to have a giant configuration, that the orbit shrinks but not into a close binary, so that it can still contain the contracting primary in thermal equilibrium. This might allow the development of a VLTP and a second common envelope event [209]. It remains to be seen if such fine tuning of the ejected envelope is statistically plausible. In this case, as the material remaining in the star undergoing the VLTP is not very large, then the expected PNe would not be very massive, but should be H-deficient. Within this picture the old H-rich PNe would be the consequence of the first common envelope, while the second H-deficient PNe would be the consequence of the second common envelope. The roundish shape observed in old H-rich PNe around most H-deficient PNe might be at odds with the expected axisymmetry of both PNe in this scenario.

Similarly in order to explain the high Ne abundances observed in the inner ejecta of Abell 58 it was suggested that an O–Ne nova might take place shortly after a final He shell flash [210]. In this scenario the initially more massive star forms a ONeMg-core WD next to a AGB companion with an intermediate separation. During the AGB the ONeMg-core WD accretes mass from the companion and, after the AGB, the post-AGB star makes a PNe in a canonical single stellar evolution fashion. Eventually, the post-AGB star experiences a VLTP flash that produces C-rich ejecta ($C/O > 1$ but relatively poor in Ne). The core idea behind this scenario is that during the final flash, the new H-deficient giant starts transferring mass to the ONeMg-core WD and this renewed accretion pushes the WD over the limit for a nova detonation. The post-AGB star then evolves in the usual post-VLTP sequence but surrounded by a mixture of the ejecta from the VLTP and the Ne nova. This Ne nova would explain the unusual Ne composition observed in the H-deficient knots of Abell 58. As in most binary evolution scenarios this requires a detailed fine tuning of both the separation of the system and the accreted masses. Moreover, under this scenario one should expect a second eruption after the VLTP observed in 1919 (V605 Aql), which was not observed [135].

5. Final words

In the previous sections we have briefly reviewed the properties of known H-deficient CSPNe and their PNe. The nature of the formation and shaping of PNe is in general is an ongoing debate, and those PNe with H-deficient CS are no exception. More crucially, evolutionary scenarios for H-deficient CSPNe and their PNe face even larger challenges, due to the diverse and exotic surface abundances and sometimes the presence of both H-rich and H-deficient PNe with different geometries.

Improving our understanding of the formation of H-deficient CSPNe and PNe will require concomitant theoretical and observational efforts. On the modeling side a better understanding of non-conservative stable and unstable mass transfer events, as well as of the common envelope stage is necessary to address the viability, and frequency, of different proposed binary scenarios. Efforts to resolve the ADF issue as well as to understand the formation and evolution of dust and gas around PNe will help to improve our understanding of the effects of binarity. Existing observing facilities such as ALMA, Gemini, the GTC and the VLTI will help accomplishing these tasks. Likewise improvements in the modeling of

AGB and post-AGB winds are needed to assess the frequency of late thermal pulses. This will require both improvements in the observational characterization of AGB and post-AGB winds, as well as an improvement in the hydrodynamical modeling of the winds.

Better, and longer, hydrodynamical simulations of the violent H-ingestion events that happen during a VLTP (and, possibly, also in white dwarf merger events) are key to improve our understanding of the born again scenario. These hydrodynamical models not only shed light on the energetics of VLTP events but are key to understand the extent of heavy element production through neutron capture processes. Quantifying the heavy-element chemical signatures of different evolutionary scenarios might be key to disentangle the contributions of each evolutionary channel and improve the comparison with observations. Moreover, using heavy element abundances to identify possible evolutionary channels requires spectroscopic analyses in the UV. Currently the best available tool for these studies is Cosmic Origins Spectrograph (COS) at the Hubble Space Telescope (HST). Due to the near-future dearth of appropriate instruments efforts should be done now to secure UV spectra for the brightest representatives of the different spectral subtypes. In addition, to extract the most information from these spectra it is necessary to improve atomic data required by state-of-the-art non-LTE model-atmosphere codes.

Further studies are needed to establish whether the shapes, sizes and locations of PNe with H-deficient central stars are statistically different from those with normal H-rich central stars. The large photometry and astrometric database from Gaia, together with ad-hoc catalogues [e.g. 31] should help resolve this issue.

We have made an effort to present both a brief pedagogical introduction and an updated view on the problem of the formation of H-deficient central stars. Regardless of our effort this review is necessarily one seen through our own spectacles and biases. We have tried to minimize this by providing as many references to the work of other authors as possible, and to mark our personal positions as such when presenting a given topic. We hope the present review serves as a starting point for those willing to study these fascinating objects and their evolution.

Funding: The author is partially funded by CONICET and Agencia I+D+i through grants PIP-2971 and PICT 2020-03316 and DAAD-CONICET (2023-2024) bilateral cooperation grant RESOL-2022-2320-APN-DIR.

Acknowledgments: M3B thanks Walter Weidmann for providing the stellar data presented in Fig. 1. M3B also thanks Alejandro Córscico, Miriam Peña, Jesús Toalá, and three anonymous referees for detailed comments and suggestions over previous versions of the manuscript that helped improving the final version of the review.

Conflicts of Interest: The author declare no conflicts of interest.

Appendix A Bona fide born again CSPNe

One of the strongest evidences in favour of the born again scenario for the formation of H-deficient CSPNe comes from few stars that have been detected during the late helium flash or immediately after. Due to the fast evolutionary speed during LTP and VLTP events capturing a star at the very moment they are undergoing a helium shell flash is rare. In spite of their rarity, these stars offer a unique opportunity to validate our theories. In particular, they show that CSPNe do evolve back to a giant configuration, and they also show how stars change their spectral types and composition during this events. Due to their importance for theories of the formation of H-deficient CSPNe here we provide a brief description of their observed properties and behaviour.

FG Sge

This variable star has shown a slow and progressive rise and of its visual magnitude from $m_{\text{photo}} = 13.6$ in 1894 to $B = 9.6$ in 1965. In turn, the spectral type of this object changed from a B5 in 1955 to A5 in 1967. From 1975 to date, both its luminosity as its color have remained approximately constant [211]. These changes can be interpreted as an

almost horizontal evolution in the HR diagram from the region of the CSPNe to the region of the yellow giants near the AGB. Indeed, [212], infer a change from $\log T_{\text{eff}} \simeq 4.65$ and $\log L/L_{\odot} \simeq 3.4$ to $\log T_{\text{eff}} \simeq 3.75$ and $\log L/L_{\odot} \simeq 4.04$ in 100 years (from 1880 to 1980). The superficial abundances of elements related to slow neutron capture processes in this star have been the subject of many discussions in the literature. These results range from the existence of changes in approximately 2 to 3 dex between 1970 to 1998 [211] to the existence of supersolar abundances, but constant from 1950 to the present [213]. During the last half century observational evidence that this object became H-deficient has accumulated. The evolution of temperature and luminosity in the last 100 years and the progressive decrease in surface abundance of H, possibly accompanied by the increase in slow neutron capture process elements, link FG Sge to the late thermal pulse scenario [213] (LTP, see Section 3). Since 1992 FG Sge shows events of abrupt decrease in luminosity, probably produced by dust condensation around the star, similar to those observed in RCrB stars.

V4334 Sgr

Yukio Sakurai reported the detection of a slow eruption in Sagittarius (V4334 Sgr) in a photograph the 20th of February of 1996. In addition, photographs taken by Sakurai during 1993 and 1994 showed no candidate at the same location, but that the star is visible on films taken in January of 1995 [214]. Benetti et al. [215] reported that both the abundances observed in a spectrum of V4334 Sgr as well as the slow evolution of luminosity make it very possible that V4334 Sgr is a star going through a VLTP, which was confirmed some days later by Duerbeck and Pollaco [216], who reported the existence of an old planetary nebula approximately 32" in diameter in that region of the sky. This led Duerbeck and Benetti [217] to propose that, indeed, V4334 Sgr was going through a VLTP episode. Photometric studies after its discovery showed V4334 Sgr increased its luminosity and cooled progressively [218], entered a stage of successive abrupt decreases in luminosity similar to those observed in RCrB stars [219], and finally disappeared behind a cloud of dust from which it has not yet emerged. Simultaneously, spectroscopic studies carried out in 1996 [220,221] showed that V4334 Sgr was suffering changes in its surface abundances, most likely due to the dredging of processed material coming from its inner regions. These studies showed that during the eruption V4334 Sgr was already a very H-deficient star, which was rich in C (both ^{12}C and ^{13}C), N, and in neutron capture elements. Analysis of the photoionization state of the nebula around V4334 Sgr by [222–224], have confirmed that V4334 Sgr was, very few years ago still a hot white dwarf star. Radio observations of V4334 Sgr carried out between 2004 and 2006 initially were interpreted as thermal emission from freshly ionized ejecta by the central star [225,226], but were later shown to be due to shock ionization [140,226]. The latest reanalysis all data from 2004 to 2023 suggests that V4334 had highly variable non-thermal emission in 2004–2017, and since 2019 has started showing an increasing contribution of thermal emission [227]. The later might be a first hint of the photoionization of the ejecta by a reheating central star. Due to the loss of the UV radiation from the CS, the old PNe around the star has started to recombine [90]. Moreover, infrared observations of the object in the last decade has shown the detection of new bipolar nebulae [89,94]. This results are in line with ALMA observations that unambiguously show the presence of an equatorial disc and bipolar outflows, formed in V4334 Sgr during the 30 years after the occurrence of the born again event [92]. This provides important constraints for future modeling efforts of this phenomenon as well as the formation of axisymmetrical structures in PNe.

In short, V4334 Sgr in the last 30 years has stopped being a hot WD to cool down and increase in brightness until it became a H-deficient yellow giant star with an RCrB type light curve, then hid from our sight in a cloud of dust in which it might be heating up again. This behavior is exactly what would be expected of an object going through a VLTP event (see Section 3), so V4334 Sgr provides the strongest observational support for the born again scenario for the formation of H-deficient stars. Moreover since the eruption

V4334 Sgr the material ejected from the star seems to have formed both bipolar outflows and an equatorial disk inside the old roundish PNe.

V605 Aql (CS of Abell 58)

This star was discovered in 1919 and was initially classified as very slow nova. Later observations, between 1919 and 1923, showed the star disappearing and reappearing at irregular intervals, similar to the observed lightcurves of RCrB stars. Based on a spectrum taken in 1921 by Lundmark [228] the star was classified as a C star. Modern inspection of the 1921 spectrum indicated that the composition of the erupting star was very similar to that of an RCrB star (with 98% He and 1% of C) [134]. In addition, many decades after the eruption, it was also recognized that the eruption took place at the center of the old PNe Abell 58 [229].

Duerbeck et al. [135] collected and studied observations of the eruption of this star between 1917 and 1923, obtaining a light curve that shows an undeniable similarity to the light curve of V4334 Sgr—which has led to V605 Aql being described as the “elder twin” of V4334 Sgr. Taking advantage of the fact that the planetary nebula that surrounds this star (Abell 58) still reflects the state of the star when it was hot enough to ionize it, photoionization studies of the nebula [136] came to the conclusion that the star, before its eruption, was a hot white dwarf star. Observations carried out in 2001, and presented by [137], show that V605 Aql is now a star with a spectrum similar to that of the CSs of planetary nebula with Wolf-Rayet spectral types ([WC]-CSPN), with He/C/O abundances 54/40/5 per mass fraction). In turn, this star now shows a much more compact He-rich nebula around it. All of these characteristics strongly indicate that V605 Aql is an object that experienced a VLTP event which turned its surface composition He-, C-, and O-rich. Consequently, V605 Aql offers a strong validation of the VLTP scenario as a channel for the formation of H-deficient CSPNe. Moreover, given the similar He-dominated composition shown by both V605 Aql and V4334 Sgr at the moment of the eruption [134,220,221] V605 Aql suggests that V4334 Sgr, whose composition at the moment of the outburst did not match that of the intershell abundances AGB stars, might soon become He-, C-, and O-rich. As in the case of V4334 Sgr, studies of the inner ejecta in the IR [230] and with ALMA [93] indicate the ejection of bipolar outflows, and the formation of axisymmetric structures after the eruption. Multiepoch optical spectroscopic observations of the H-deficient ejecta around V605 Aql shows that the ejecta has experienced significant brightening from 1996 to 2021. These changes have been attributed to shocks in the bipolar H-deficient outflow [231]. Integral field spectroscopic observations obtained in 2022 using MEGARA at the GTC, in combination with ALMA and Hubble Space Telescope data, lead [232] to propose very complex structure around V605 Aql. The structure consists of an hourglass structure for the ionized material, around a high-velocity polar component together with an expanding toroidal molecular and dusty structure. Such complex structure has been interpreted by [232] as a proof of the presence of an unseen close stellar or sub-stellar companion.

Hen 3-1357, SAO 244567 (CS of the Stingray PN)

First reported in 1970 as a B type star [233], Hen 3-1357 was recognized in 1993 as a very fast evolving star [234]. Based on the optical spectrum, and its UBV colours, it was concluded that Hen 3-1357 had an effective temperature of $T_{\text{eff}} \simeq 21$ kK in 1971 [234,235]. Optical and ultraviolet spectra between 1990 and 1992 revealed that Hen 3-1357 had ionized its surrounding nebula within only two decades (the Stingray Nebula) [234,235]. Reindl et al. [236], presented first quantitative spectral analyses of all available spectra and found that the CS had increased its T_{eff} from 38000 K in 1988 to a peak value of 60000 K in 2002. During this period its surface gravity increased continuously from $\log g = 4.8$ to $\log g = 6$, which implies a significant drop in luminosity. In a follow up study, these authors [147] found that Hen 3-1357, after the initial rapid heating and contraction, had cooled and expanded significantly from 2002 to 2006, reaching values of $T_{\text{eff}} = 50000$ K and $\log g = 5.5$ in 2006. These observations confirmed the suspicion that Hen 3-1357 is undergoing a LTP, as

such change in the evolution of the effective temperature and gravity can only be explained within the LTP scenario. The sudden change in the evolution of the star due to the late He flash is also notable in the lightcurve of the star, which shows a steady decline from 1889 to 1980, followed by a sudden fast fading from 1980 to 2006 [237]. The evolutionary speed suggested a CS mass between 0.53 and 0.56 M_{\odot} [147]. However, none of the current LTP models can fully reproduce the evolution of all characteristics of the star [122,147]. The comparison of the nebular abundances with those predicted by stellar evolution and nucleosynthesis models at the end of the AGB phase suggest that the CS had an initial mass lower than 1.5 M_{\odot} . The sudden cooling of the CS was followed by large decreases in its nebular emission-line fluxes. It has been now confirmed that the nebula is recombining due to the disappearance of the ionizing source [238,239]. From the analysis of the physical conditions of the nebulae some authors concluded that the effective temperature of Hen 3-1357 has decreased from about 60000 K in 2002 to less than 40000 K in 2021 [238].

Based on our understanding of the scenario we expect Hen 3-1357 to continue cooling for some decades, reaching a giant configuration again. Whether this star will become H-deficient or not in the future depends on whether third dredge up events take place once the star is back on the AGB, something that depends strongly on the mass of the CS and on the physics of CBM which is not well understood at the moment (see Section 3).

Other stars discussed in connection with the born again scenario

In addition to the objects mentioned above, other stars/eruptions have been mentioned in connection with the born again scenario. Among them V838 Monocerotis, CK Vul, and NSV43434 have been discussed as possible born again events [148,240,241], but were later shown to be novae, stellar mergers or other types of stellar transients [242–246]. Moreover, the central star HuBi 1 has been identified by some studies as evolving fast through the HR diagram after a VLTP event [88,171,247,248], although this interpretation is still under debate and alternative interpretations have been suggested [84,95,249].

References

- Messier, C. Catalogue des Nébuleuses et des Amas d'Étoiles (Catalog of Nebulae and Star Clusters). *Connaissance des Temps ou des Mouvements Célestes*, for 1784, p. 227–267, 1781.
- Shklovsky, I.S. The nature of planetary nebulae and their nuclei. *Astronomicheskii Zhurnal* **1956**, *33*, 315–329.
- Abell, G.O.; Goldreich, P. On the Origin of Planetary Nebulae. *PASP* **1966**, *78*, 232. <https://doi.org/10.1086/128336>.
- Paczyński, B. Evolution of Single Stars. I. Stellar Evolution from Main Sequence to White Dwarf or Carbon Ignition. *Acta Astronomica* **1970**, *20*, 47.
- Paczyński, B. Evolution of Single Stars. VI. Model Nuclei of Planetary Nebulae. *Acta Astronomica* **1971**, *21*, 417.
- Kwok, S.; Purton, C.R.; Fitzgerald, P.M. On the origin of planetary nebulae. *ApJL* **1978**, *219*, L125–L127. <https://doi.org/10.1086/182621>.
- Kahn, F.D.; West, K.A. Shapes of planetary nebulae. *MNRAS* **1985**, *212*, 837–850. <https://doi.org/10.1093/mnras/212.4.837>.
- Bond, H.E. Binariness of Central Stars of Planetary Nebulae. In Proceedings of the Asymmetrical Planetary Nebulae II: From Origins to Microstructures; Kastner, J.H.; Soker, N.; Rappaport, S., Eds., 2000, Vol. 199, *Astronomical Society of the Pacific Conference Series*, p. 115, [arXiv:astro-ph/9909516].
- Balick, B.; Frank, A. Shapes and Shaping of Planetary Nebulae. *ARA&A* **2002**, *40*, 439–486. <https://doi.org/10.1146/annurev.astro.40.060401.093849>.
- De Marco, O. The Origin and Shaping of Planetary Nebulae: Putting the Binary Hypothesis to the Test. *PASP* **2009**, *121*, 316, [arXiv:astro-ph.GA/0902.1137]. <https://doi.org/10.1086/597765>.
- Jones, D.; Boffin, H.M.J. Binary stars as the key to understanding planetary nebulae. *Nature Astronomy* **2017**, *1*, 0117, [arXiv:astro-ph.SR/1705.00283]. <https://doi.org/10.1038/s41550-017-0117>.
- Boffin, H.M.J.; Jones, D. *The Importance of Binaries in the Formation and Evolution of Planetary Nebulae*; 2019. <https://doi.org/10.1007/978-3-030-25059-1>.
- Miszalski, B.; Acker, A.; Parker, Q.A.; Moffat, A.F.J. Binary planetary nebulae nuclei towards the Galactic bulge. II. A penchant for bipolarity and low-ionisation structures. *A&A* **2009**, *505*, 249–263, [arXiv:astro-ph.SR/0907.2463]. <https://doi.org/10.1051/0004-6361/200912176>.
- Miszalski, B.; Acker, A.; Moffat, A.F.J.; Parker, Q.A.; Udalski, A. Binary planetary nebulae nuclei towards the Galactic bulge. I. Sample discovery, period distribution, and binary fraction. *A&A* **2009**, *496*, 813–825, [arXiv:astro-ph.SR/0901.4419]. <https://doi.org/10.1051/0004-6361/200811380>.

15. Jacoby, G.H.; Hillwig, T.C.; Jones, D.; Martin, K.; De Marco, O.; Kronberger, M.; Hurowitz, J.L.; Crocker, A.F.; Dey, J. Binary central stars of planetary nebulae identified with Kepler/K2. *MNRAS* **2021**, *506*, 5223–5246, [arXiv:astro-ph.SR/2104.07934]. <https://doi.org/10.1093/mnras/stab2045>.
16. Douchin, D.; De Marco, O.; Frew, D.J.; Jacoby, G.H.; Jasniewicz, G.; Fitzgerald, M.; Passy, J.C.; Harmer, D.; Hillwig, T.; Moe, M. The binary fraction of planetary nebula central stars - II. A larger sample and improved technique for the infrared excess search. *MNRAS* **2015**, *448*, 3132–3155. <https://doi.org/10.1093/mnras/stu2700>.
17. Adam, C.; Mugrauer, M. HIP 3678: a hierarchical triple stellar system in the centre of the planetary nebula NGC 246. *MNRAS* **2014**, *444*, 3459–3465, [arXiv:astro-ph.SR/1409.5339]. <https://doi.org/10.1093/mnras/stu1677>.
18. De Marco, O.; Akashi, M.; Akras, S.; Alcolea, J.; Aleman, I.; Amram, P.; Balick, B.; De Beck, E.; Blackman, E.G.; Boffin, H.M.J.; et al. The messy death of a multiple star system and the resulting planetary nebula as observed by JWST. *Nature Astronomy* **2022**, *6*, 1421–1432, [arXiv:astro-ph.SR/2301.02775]. <https://doi.org/10.1038/s41550-022-01845-2>.
19. Hillwig, T.C.; Bond, H.E.; Afşar, M.; De Marco, O. Binary Central Stars of Planetary Nebulae Discovered Through Photometric Variability. II. Modeling the Central Stars of NGC 6026 and NGC 6337. *AJ* **2010**, *140*, 319–327. <https://doi.org/10.1088/0004-6256/140/2/319>.
20. Tovmassian, G.; Yungelson, L.; Rauch, T.; Suleimanov, V.; Napiwotzki, R.; Stasińska, G.; Tomsick, J.; Wilms, J.; Morisset, C.; Peña, M.; et al. The Double-degenerate Nucleus of the Planetary Nebula TS 01: A Close Binary Evolution Showcase. *ApJ* **2010**, *714*, 178–193, [arXiv:astro-ph.SR/1003.0639]. <https://doi.org/10.1088/0004-637X/714/1/178>.
21. Reindl, N.; Schaffenroth, V.; Miller Bertolami, M.M.; Geier, S.; Finch, N.L.; Barstow, M.A.; Casewell, S.L.; Taubenberger, S. An in-depth reanalysis of the alleged type Ia supernova progenitor Henize 2-428. *A&A* **2020**, *638*, A93, [arXiv:astro-ph.SR/2006.14688]. <https://doi.org/10.1051/0004-6361/202038117>.
22. Hillwig, T.C.; Reindl, N.; Rotter, H.M.; Rengstorf, A.W.; Heber, U.; Irrgang, A. Two evolved close binary stars: GALEX J015054.4+310745 and the central star of the planetary nebula Hen 2-84. *MNRAS* **2022**, *511*, 2033–2039. <https://doi.org/10.1093/mnras/stac226>.
23. Jacob, R.; Schönberner, D.; Steffen, M. The evolution of planetary nebulae. VIII. True expansion rates and visibility times. *A&A* **2013**, *558*, A78, [arXiv:astro-ph.SR/1307.6189]. <https://doi.org/10.1051/0004-6361/201321532>.
24. Kwitter, K.B.; Henry, R.B.C. Planetary Nebulae: Sources of Enlightenment. *PASP* **2022**, *134*, 022001, [arXiv:astro-ph.SR/2110.13993]. <https://doi.org/10.1088/1538-3873/ac32b1>.
25. Kwok, S. *The Origin and Evolution of Planetary Nebulae*; 2000.
26. van der Hucht, K.A.; Conti, P.S.; Lundstrom, I.; Stenholm, B. The Sixth Catalogue of Galactic Wolf-Rayet Stars - Their Past and Present. *Space Science Reviews* **1981**, *28*, 227–306. <https://doi.org/10.1007/BF00173260>.
27. Aller, L.H.; Wilson, O.C. Spectrophotometry of the Central Stars of Four Planetary Nebulae. *ApJ* **1954**, *119*, 243. <https://doi.org/10.1086/145816>.
28. Aller, L.H.; Liller, W. Planetary Nebulae. In *Nebulae and Interstellar Matter*; Middlehurst, B.M.; Aller, L.H., Eds.; 1968; p. 483.
29. Heap, S.R. Spectroscopic studies of very old hot stars. I. NGC 246 and its exciting star. *ApJ* **1975**, *196*, 195. <https://doi.org/10.1086/153405>.
30. Wesemael, F.; Green, R.F.; Liebert, J. Spectrophotometric and model-atmosphere analyses of the hot DO and DAO white dwarfs from the Palomar-Green survey. *ApJS* **1985**, *58*, 379–411. <https://doi.org/10.1086/191046>.
31. Weidmann, W.A.; Mari, M.B.; Schmidt, E.O.; Gaspar, G.; Miller Bertolami, M.M.; Oio, G.A.; Gutiérrez-Soto, L.A.; Volpe, M.G.; Gamen, R.; Mast, D. Catalogue of the central stars of planetary nebulae. Expanded edition. *A&A* **2020**, *640*, A10, [arXiv:astro-ph.GA/2005.10368]. <https://doi.org/10.1051/0004-6361/202037998>.
32. Werner, K.; Heber, U.; Hunger, K. Non-Lte Spectral Analysis of PG:1159-035 Stars. In *IAU Colloq. 114: White Dwarfs*; Wegner, G., Ed.; 1989; Vol. 328, p. 194. https://doi.org/10.1007/3-540-51031-1_317.
33. Werner, K.; Heber, U. On the evolutionary link between white dwarfs and central stars of planetary nebulae : NLTE analysis of PG 1144+005. *A&A* **1991**, *247*, 476.
34. Leuenhagen, U.; Hamann, W.R. V348 Sagittarii : analysis of the [WC12] stellar spectrum. *A&A* **1994**, *283*, 567–581.
35. Leuenhagen, U.; Hamann, W.R.; Jeffery, C.S. Spectral analyses of late-type WC central stars of planetary nebulae. *A&A* **1996**, *312*, 167–185.
36. Leuenhagen, U.; Hamann, W.R. Spectral analyses of late-type [WC] central stars of planetary nebulae: more empirical constraints for their evolutionary status. *A&A* **1998**, *330*, 265–276.
37. Werner, K.; Herwig, F. The Elemental Abundances in Bare Planetary Nebula Central Stars and the Shell Burning in AGB Stars. *PASP* **2006**, *118*, 183–204, [arXiv:astro-ph/astro-ph/0512320]. <https://doi.org/10.1086/500443>.
38. Iben, I., Jr.; Kaler, J.B.; Truran, J.W.; Renzini, A. On the evolution of those nuclei of planetary nebulae that experience a final helium shell flash. *ApJ* **1983**, *264*, 605–612. <https://doi.org/10.1086/160631>.
39. Iben, I., Jr. On the frequency of planetary nebula nuclei powered by helium burning and on the frequency of white dwarfs with hydrogen-deficient atmospheres. *ApJ* **1984**, *277*, 333–354. <https://doi.org/10.1086/161700>.
40. Mendez, R.H.; Miguel, C.H.; Heber, U.; Kudritzki, R.P. Helium Rich Subdwarf 0 Stars and Central Stars of Planetary Nebulae (review). In *Proceedings of the IAU Colloq. 87: Hydrogen Deficient Stars and Related Objects*; Hunger, K.; Schoenberner, D.; Kameswara Rao, N., Eds., 1986, p. 323. https://doi.org/10.1007/978-94-009-4744-3_27.

41. Mendez, R.H. Photospheric Abundances in Central Stars of Planetary Nebulae, and Evolutionary Implications. In Proceedings of the Evolution of Stars: the Photospheric Abundance Connection; Michaud, G.; Tutukov, A.V., Eds., 1991, Vol. 145, p. 375.
42. Rauch, T.; Dreizler, S.; Wolff, B. Spectral analysis of O(He)-type post-AGB stars. *A&A* **1998**, *338*, 651–660.
43. Miszalski, B.; Crowther, P.A.; De Marco, O.; Köppen, J.; Moffat, A.F.J.; Acker, A.; Hillwig, T.C. IC 4663: the first unambiguous [WN] Wolf-Rayet central star of a planetary nebula. *MNRAS* **2012**, *423*, 934–947, [arXiv:astro-ph.SR/1203.3303]. <https://doi.org/10.1111/j.1365-2966.2012.20929.x>.
44. Jeffery, C.S. Hydrogen-Deficient Stars and Stellar Systems. In Proceedings of the Proceedings of a CCP7 Workshop: Hydrogen-deficient stellar systems; Jeffery, C.S., Ed., 1994.
45. Jeffery, C.S. Hydrogen-Deficient Stars: An Introduction. In Proceedings of the Hydrogen-Deficient Stars; Werner, A.; Rauch, T., Eds., 2008, Vol. 391, *Astronomical Society of the Pacific Conference Series*, p. 3.
46. Rauch, T.; Reiff, E.; Werner, K.; Herwig, F.; Koesterke, L.; Kruk, J.W. On the Evolutionary Status of Extremely Hot Helium Stars — are O(He) Stars Successors of RCrB Stars? In Proceedings of the Astrophysics in the Far Ultraviolet: Five Years of Discovery with FUSE; Sonneborn, G.; Moos, H.W.; Andersson, B.G., Eds., 2006, Vol. 348, *Astronomical Society of the Pacific Conference Series*, p. 194.
47. Reindl, N.; Rauch, T.; Werner, K.; Kruk, J.W.; Todt, H. On helium-dominated stellar evolution: the mysterious role of the O(He)-type stars. *A&A* **2014**, *566*, A116, [arXiv:astro-ph.SR/1405.1589]. <https://doi.org/10.1051/0004-6361/201423498>.
48. DePew, K.; Parker, Q.A.; Miszalski, B.; De Marco, O.; Frew, D.J.; Acker, A.; Kovacevic, A.V.; Sharp, R.G. Newly discovered Wolf-Rayet and weak emission-line central stars of planetary nebulae. *MNRAS* **2011**, *414*, 2812–2827, [arXiv:astro-ph.SR/1101.2468]. <https://doi.org/10.1111/j.1365-2966.2011.18337.x>.
49. Todt, H.; Kniazev, A.Y.; Gvaramadze, V.V.; Hamann, W.R.; Buckley, D.; Crause, L.; Crawford, S.M.; Gulbis, A.A.S.; Hettlage, C.; Hooper, E.; et al. Abell 48 - a rare WN-type central star of a planetary nebula. *MNRAS* **2013**, *430*, 2302–2312, [arXiv:astro-ph.SR/1301.1944]. <https://doi.org/10.1093/mnras/stt056>.
50. Frew, D.J.; Bojčić, I.S.; Parker, Q.A.; Stupar, M.; Wachter, S.; DePew, K.; Danehkar, A.; Fitzgerald, M.T.; Douchin, D. The planetary nebula Abell 48 and its [WN] nucleus. *MNRAS* **2014**, *440*, 1345–1364, [arXiv:astro-ph.SR/1301.3994]. <https://doi.org/10.1093/mnras/stu198>.
51. Acker, A.; Neiner, C. Quantitative classification of WR nuclei of planetary nebulae. *A&A* **2003**, *403*, 659–673. <https://doi.org/10.1051/0004-6361:20030391>.
52. Todt, H.; Peña, M.; Hamann, W.R.; Gräfener, G. The central star of the planetary nebula PB 8: a Wolf-Rayet-type wind of an unusual WN/WC chemical composition. *A&A* **2010**, *515*, A83, [arXiv:astro-ph.SR/1003.3419]. <https://doi.org/10.1051/0004-6361/200912183>.
53. Löbbling, L.; Rauch, T.; Miller Bertolami, M.M.; Todt, H.; Friederich, F.; Ziegler, M.; Werner, K.; Kruk, J.W. Spectral analysis of the hybrid PG 1159-type central stars of the planetary nebulae Abell 43 and NGC 7094. *MNRAS* **2019**, *489*, 1054–1071, [arXiv:astro-ph.SR/1907.07049]. <https://doi.org/10.1093/mnras/stz1994>.
54. Werner, K.; Rauch, T.; Kepler, S.O. New hydrogen-deficient (pre-) white dwarfs in the Sloan Digital Sky Survey Data Release 10. *A&A* **2014**, *564*, A53. <https://doi.org/10.1051/0004-6361/201423441>.
55. Todt, H.; Hamann, W.R. Wolf-Rayet central stars of planetary nebulae. In Proceedings of the Wolf-Rayet Stars; Hamann, W.R.; Sander, A.; Todt, H., Eds., 2015, pp. 253–258.
56. Miller Bertolami, M.M.; Althaus, L.G.; Serenelli, A.M.; Panei, J.A. New evolutionary calculations for the born again scenario. *A&A* **2006**, *449*, 313–326, [arXiv:astro-ph/astro-ph/0511406]. <https://doi.org/10.1051/0004-6361:20053804>.
57. Miller Bertolami, M.M.; Althaus, L.G. Full evolutionary models for PG 1159 stars. Implications for the helium-rich O(He) stars. *A&A* **2006**, *454*, 845–854, [arXiv:astro-ph/astro-ph/0603846]. <https://doi.org/10.1051/0004-6361:20054723>.
58. Miller Bertolami, M.M.; Althaus, L.G. The born-again (very late thermal pulse) scenario revisited: the mass of the remnants and implications for V4334 Sgr. *MNRAS* **2007**, *380*, 763–770, [arXiv:astro-ph/0706.0714]. <https://doi.org/10.1111/j.1365-2966.2007.12115.x>.
59. McGraw, J.T.; Starrfield, S.G.; Liebert, J.; Green, R. PG 1159-035: a New, Hot, Non-Da Pulsating Degenerate. In Proceedings of the IAU Colloq. 53: White Dwarfs and Variable Degenerate Stars; van Horn, H.M.; Weidemann, V.; Savedoff, M.P., Eds., 1979, p. 377.
60. Grauer, A.D.; Bond, H.E. The pulsating central star of the planetary nebula Kohoutek 1-16. *ApJ* **1984**, *277*, 211–215. <https://doi.org/10.1086/161685>.
61. Córscico, A.H.; Althaus, L.G.; Miller Bertolami, M.M.; Kepler, S.O. Pulsating white dwarfs: new insights. *A&ARev* **2019**, *27*, 7, [arXiv:astro-ph.SR/1907.00115]. <https://doi.org/10.1007/s00159-019-0118-4>.
62. Córscico, A.H. White-dwarf asteroseismology with the Kepler space telescope. *Frontiers in Astronomy and Space Sciences* **2020**, *7*, 47, [arXiv:astro-ph.SR/2006.04955]. <https://doi.org/10.3389/fspas.2020.00047>.
63. Córscico, A.H.; Althaus, L.G.; Miller Bertolami, M.M.; Werner, K. Asteroseismological constraints on the pulsating planetary nebula nucleus (PG 1159-type) RX J2117.1+3412. *A&A* **2007**, *461*, 1095–1102, [arXiv:astro-ph/astro-ph/0610420]. <https://doi.org/10.1051/0004-6361:20066452>.
64. Córscico, A.H.; Miller Bertolami, M.M.; Althaus, L.G.; Vaclair, G.; Werner, K. Asteroseismological constraints on the coolest GW Virginis variable star (PG 1159-type) <ASTROBJ>PG 0122+200</ASTROBJ>. *A&A* **2007**, *475*, 619–627, [arXiv:astro-ph/0709.0280]. <https://doi.org/10.1051/0004-6361:20078145>.
65. Althaus, L.G.; Córscico, A.H.; Kepler, S.O.; Miller Bertolami, M.M. On the systematics of asteroseismological mass determinations of PG 1159 stars. *A&A* **2008**, *478*, 175–180, [arXiv:astro-ph/0710.3394]. <https://doi.org/10.1051/0004-6361:20078524>.

66. Córscico, A.H.; Althaus, L.G.; Kepler, S.O.; Costa, J.E.S.; Miller Bertolami, M.M. Asteroseismological measurements on PG 1159-035, the prototype of the GW Virginis variable stars. *A&A* **2008**, *478*, 869–881, [arXiv:astro-ph/0712.0795]. <https://doi.org/10.1051/0004-6361:20078646>.
67. Córscico, A.H.; Althaus, L.G.; Miller Bertolami, M.M.; García-Berro, E. Asteroseismology of hot pre-white dwarf stars: the case of the DOV stars PG 2131+066 and PG 1707+427, and the PNNV star NGC 1501. *A&A* **2009**, *499*, 257–266, [arXiv:astro-ph.SR/0903.3628]. <https://doi.org/10.1051/0004-6361/200810727>.
68. Córscico, A.H.; Uzundag, M.; Kepler, S.O.; Althaus, L.G.; Silvotti, R.; Baran, A.S.; Vučković, M.; Werner, K.; Bell, K.J.; Higgins, M. Pulsating hydrogen-deficient white dwarfs and pre-white dwarfs observed with TESS. I. Asteroseismology of the GW Vir stars RX J2117+3412, HS 2324+3944, NGC 6905, NGC 1501, NGC 2371, and K 1-16. *A&A* **2021**, *645*, A117, [arXiv:astro-ph.SR/2011.03629]. <https://doi.org/10.1051/0004-6361/202039202>.
69. Calcaferro, L.M.; Sowicka, P.; Uzundag, M.; Córscico, A.H.; Kepler, S.O.; Bell, K.J.; Althaus, L.G.; Handler, G.; Kawaler, S.D.; Werner, K. Pulsating hydrogen-deficient white dwarfs and pre-white dwarfs observed with TESS. VI. Asteroseismology of the GW Vir-type central star of the Planetary Nebula NGC 246. *A&A* **2024**, *686*, A140, [arXiv:astro-ph.SR/2402.16642]. <https://doi.org/10.1051/0004-6361/202349103>.
70. Charpinet, S.; Fontaine, G.; Brassard, P. Seismic evidence for the loss of stellar angular momentum before the white-dwarf stage. *Nature* **2009**, *461*, 501–503. <https://doi.org/10.1038/nature08307>.
71. Córscico, A.H.; Althaus, L.G.; Kawaler, S.D.; Miller Bertolami, M.M.; García-Berro, E.; Kepler, S.O. Probing the internal rotation of pre-white dwarf stars with asteroseismology: the case of PG 0122+200. *MNRAS* **2011**, *418*, 2519–2526, [arXiv:astro-ph.SR/1108.3359]. <https://doi.org/10.1111/j.1365-2966.2011.19642.x>.
72. Serenelli, A.; Weiss, A.; Aerts, C.; Angelou, G.C.; Baroch, D.; Bastian, N.; Beck, P.G.; Bergemann, M.; Bestenlehner, J.M.; Czekala, I.; et al. Weighing stars from birth to death: mass determination methods across the HRD. *A&ARev* **2021**, *29*, 4, [arXiv:astro-ph.SR/2006.10868]. <https://doi.org/10.1007/s00159-021-00132-9>.
73. Córscico, A.H.; Althaus, L.G. Can pulsating PG 1159 stars place constraints on the occurrence of core overshooting? *A&A* **2005**, *439*, L31–L34, [arXiv:astro-ph/astro-ph/0507255]. <https://doi.org/10.1051/0004-6361:200500154>.
74. Althaus, L.G.; Córscico, A.H.; Miller Bertolami, M.M.; García-Berro, E.; Kepler, S.O. Evidence of Thin Helium Envelopes in PG 1159 Stars. *ApJL* **2008**, *677*, L35, [arXiv:astro-ph/0802.3363]. <https://doi.org/10.1086/587739>.
75. Zijlstra, A.A. Hydrogen-poor planetary nebulae. *Ap&SS* **2002**, *279*, 171–182, [arXiv:astro-ph/astro-ph/0105448]. <https://doi.org/10.48550/arXiv.astro-ph/0105448>.
76. Hazard, C.; Terlevich, R.; Morton, D.C.; Sargent, W.L.W.; Ferland, G. Evidence for highly processed material ejected from Abell 30. *Nature* **1980**, *285*, 463–464. <https://doi.org/10.1038/285463a0>.
77. Jacoby, G.H.; Ford, H.C. The hydrogen-depleted planetary nebulae Abell 30 and Abell 78. *ApJ* **1983**, *266*, 298–308. <https://doi.org/10.1086/160779>.
78. Seitter, W.C. V 605 Aquilae - A star and a nebula with no hydrogen. *The Messenger* **1987**, *50*, 14–17.
79. Gillett, F.C.; Jacoby, G.H.; Joyce, R.R.; Cohen, J.G.; Neugebauer, G.; Soifer, B.T.; Nakajima, T.; Matthews, K. The Optical/Infrared Counterpart(s) of IRAS 18333-2357. *ApJ* **1989**, *338*, 862. <https://doi.org/10.1086/167241>.
80. Cohen, J.G.; Gillett, F.C. The Peculiar Planetary Nebula in M22. *ApJ* **1989**, *346*, 803. <https://doi.org/10.1086/168061>.
81. Machado, A.; Garcia-Lario, P.; Pottasch, S.R. IRAS 16455-3455 and IRAS 15154-5258 : two new southern planetary nebulae. *A&A* **1989**, *218*, 267–272.
82. Kerber, F.; Pirzkal, N.; De Marco, O.; Asplund, M.; Clayton, G.C.; Rosa, M.R. Freshly Ionized Matter around the Final Helium Shell Flash Object V4334 Sagittarii (Sakurai's Object). *ApJL* **2002**, *581*, L39–L42, [arXiv:astro-ph/astro-ph/0211275]. <https://doi.org/10.1086/345773>.
83. Gvaramadze, V.V.; Kniazev, A.Y.; Gräfener, G.; Langer, N. WR 72: a born-again planetary nebula with hydrogen-poor knots. *MNRAS* **2020**, *492*, 3316–3322, [arXiv:astro-ph.SR/1912.11051]. <https://doi.org/10.1093/mnras/stz3639>.
84. Montoro-Molina, B.; Guerrero, M.A.; Pérez-Díaz, B.; Toalá, J.A.; Cazzoli, S.; Miller Bertolami, M.M.; Morisset, C. Chemistry and physical properties of the born-again planetary nebula HuBi 1. *MNRAS* **2022**, *512*, 4003–4020, [arXiv:astro-ph.SR/2202.00353]. <https://doi.org/10.1093/mnras/stac336>.
85. Muthumariappan, C. Three-dimensional Monte Carlo dust radiative transfer study of the H-poor planetary nebula IRAS 18333-2357 located in M22. *MNRAS* **2017**, *470*, 626–638. <https://doi.org/10.1093/mnras/stx1071>.
86. Harrington, J.P. Observations and models of H-deficient planetary nebulae. In Proceedings of the Hydrogen Deficient Stars; Jeffery, C.S.; Heber, U., Eds., 1996, Vol. 96, *Astronomical Society of the Pacific Conference Series*, p. 193.
87. Rechy-García, J.S.; Guerrero, M.A.; Santamaría, E.; Gómez-González, V.M.A.; Ramos-Larios, G.; Toalá, J.A.; Cazzoli, S.; Sabin, L.; Miranda, L.F.; Fang, X.; et al. Discovery of a Fast-expanding Shell in the Inside-out Born-again Planetary Nebula HuBi 1 through High-dispersion Integral Field Spectroscopy. *ApJL* **2020**, *903*, L4, [arXiv:astro-ph.SR/2009.13575]. <https://doi.org/10.3847/2041-8213/abbe22>.
88. Rodríguez-González, A.; Peña, M.; Hernández-Martínez, L.; Ruiz-Escobedo, F.; Raga, A.; Stasińska, G.; Castorena, J.I. Numerical Models of Planetary Nebulae with Different Episodes of Mass Ejection: The Particular Case of HuBi 1. *ApJ* **2023**, *955*, 151, [arXiv:astro-ph.GA/2308.13190]. <https://doi.org/10.3847/1538-4357/acf0bc>.
89. Hinkle, K.H.; Joyce, R.R. The Spatially Resolved Bipolar Nebula of Sakurai's Object. *ApJ* **2014**, *785*, 146. <https://doi.org/10.1088/0004-637X/785/2/146>.

90. Reichel, M.; Kimeswenger, S.; van Hoof, P.A.M.; Zijlstra, A.A.; Barría, D.; Hajduk, M.; Van de Steene, G.C.; Tafuya, D. Re-combination of Hot Ionized Nebulae: The Old Planetary Nebula around V4334 Sgr (Sakurai's Star). *ApJ* **2022**, *939*, 103, [arXiv:astro-ph.SR/2209.03634]. <https://doi.org/10.3847/1538-4357/ac90c4>.
91. Rodríguez-González, J.B.; Santamaría, E.; Toalá, J.A.; Guerrero, M.A.; Montoro-Molina, B.; Rubio, G.; Tafuya, D.; Chu, Y.H.; Ramos-Larios, G.; Sabin, L. Common envelope evolution in born-again planetary nebulae - Shaping the H-deficient ejecta of A 30. *MNRAS* **2022**, *514*, 4794–4802.
92. Tafuya, D.; van Hoof, P.A.M.; Toalá, J.A.; Van de Steene, G.; Randall, S.; Unnikrishnan, R.; Kimeswenger, S.; Hajduk, M.; Barría, D.; Zijlstra, A. The heart of Sakurai's object revealed by ALMA. *A&A* **2023**, *677*, L8, [arXiv:astro-ph.SR/2308.08962]. <https://doi.org/10.1051/0004-6361/202347293>.
93. Tafuya, D.; Toalá, J.A.; Unnikrishnan, R.; Vlemmings, W.H.T.; Guerrero, M.A.; Kimeswenger, S.; van Hoof, P.A.M.; Zapata, L.A.; Treviño-Morales, S.P.; Rodríguez-González, J.B. First Images of the Molecular Gas around a Born-again Star Revealed by ALMA. *ApJL* **2022**, *925*, L4, [arXiv:astro-ph.GA/2201.04110]. <https://doi.org/10.3847/2041-8213/ac4a5b>.
94. Hinkle, K.H.; Joyce, R.R.; Matheson, T.; Lacy, J.H.; Richter, M.J. The Spatially Resolved Bipolar Nebula of Sakurai's Object. II. Mapping the Planetary Nebula Expansion. *ApJ* **2020**, *904*, 34. <https://doi.org/10.3847/1538-4357/abbd9a>.
95. Guerrero, M.A.; Fang, X.; Miller Bertolami, M.M.; Ramos-Larios, G.; Todt, H.; Alarie, A.; Sabin, L.; Miranda, L.F.; Morisset, C.; Kehrig, C.; et al. The inside-out planetary nebula around a born-again star. *Nature Astronomy* **2018**, *2*, 784–789, [arXiv:astro-ph.SR/1808.03462]. <https://doi.org/10.1038/s41550-018-0551-8>.
96. Wyse, A.B. The Spectra of Ten Gaseous Nebulae. *ApJ* **1942**, *95*, 356. <https://doi.org/10.1086/144409>.
97. Wesson, R.; Barlow, M.J.; Liu, X.W.; Storey, P.J.; Ercolano, B.; De Marco, O. The hydrogen-deficient knot of the 'born-again' planetary nebula Abell 58 (V605 Aql). *MNRAS* **2008**, *383*, 1639–1648, [arXiv:astro-ph/0711.1139]. <https://doi.org/10.1111/j.1365-2966.2007.12683.x>.
98. Simpson, J.; Jones, D.; Wesson, R.; García-Rojas, J. Abundance Analysis of the J4 Equatorial Knot of the Born-again Planetary Nebula A30. *Research Notes of the American Astronomical Society* **2022**, *6*, 4, [arXiv:astro-ph.SR/2201.05627]. <https://doi.org/10.3847/2515-5172/ac47a6>.
99. Wesson, R.; Liu, X.W.; Barlow, M.J. Physical conditions in the planetary nebula Abell 30. *MNRAS* **2003**, *340*, 253–263, [arXiv:astro-ph/astro-ph/0301119]. <https://doi.org/10.1046/j.1365-8711.2003.06289.x>.
100. Wesson, R.; Jones, D.; García-Rojas, J.; Boffin, H.M.J.; Corradi, R.L.M. Confirmation of the link between central star binarity and extreme abundance discrepancy factors in planetary nebulae. *MNRAS* **2018**, *480*, 4589–4613, [arXiv:astro-ph.SR/1807.09272]. <https://doi.org/10.1093/mnras/sty1871>.
101. Liu, X.W. Probing the Dark Secrets of PNe with ORLs (invited review). In Proceedings of the Planetary Nebulae: Their Evolution and Role in the Universe; Kwok, S.; Dopita, M.; Sutherland, R., Eds., 2003, Vol. 209, *IAU Symposium*, p. 339.
102. Jacoby, G.H.; Hillwig, T.C.; Jones, D. Abell 30 - A binary central star among the born-again planetary nebulae. *MNRAS* **2020**, *498*, L114–L118, [arXiv:astro-ph.SR/2008.01488]. <https://doi.org/10.1093/mnras/51/1/laa138>.
103. Kippenhahn, R.; Weigert, A.; Weiss, A. *Stellar Structure and Evolution*; 2013. <https://doi.org/10.1007/978-3-642-30304-3>.
104. Kippenhahn, R.; Weigert, A.; Weiss, A. *Stellar Structure and Evolution*; 2012. <https://doi.org/10.1007/978-3-642-30304-3>.
105. Karakas, A.I.; Lattanzio, J.C. The Dawes Review 2: Nucleosynthesis and Stellar Yields of Low- and Intermediate-Mass Single Stars. *PASA* **2014**, *31*, e030, [arXiv:astro-ph.SR/1405.0062]. <https://doi.org/10.1017/pasa.2014.21>.
106. Höfner, S.; Olofsson, H. Mass loss of stars on the asymptotic giant branch. Mechanisms, models and measurements. *A&ARev* **2018**, *26*, 1. <https://doi.org/10.1007/s00159-017-0106-5>.
107. Marigo, P. Asymptotic Giant Branch evolution at varying surface C/O ratio: effects of changes in molecular opacities. *A&A* **2002**, *387*, 507–519, [arXiv:astro-ph/astro-ph/0203036]. <https://doi.org/10.1051/0004-6361:20020304>.
108. Schoenberner, D. Asymptotic giant branch evolution with steady mass loss. *A&A* **1979**, *79*, 108–114.
109. Blöcker, T. Evolution on the AGB and beyond: on the formation of H-deficient post-AGB stars. *Ap&SS* **2001**, *275*, 1–14, [arXiv:astro-ph/astro-ph/0102135]. <https://doi.org/10.1023/A:1002777931450>.
110. Iben, I., J.; MacDonald, J. The Born Again AGB Phenomenon. In *White Dwarfs*; Koester, D.; Werner, K., Eds.; 1995; Vol. 443, p. 48.
111. Iben, I., J. Further adventures of a thermally pulsating star. *ApJ* **1976**, *208*, 165–176. <https://doi.org/10.1086/154591>.
112. Herwig, F.; Pignatari, M.; Woodward, P.R.; Porter, D.H.; Rockefeller, G.; Fryer, C.L.; Bennett, M.; Hirschi, R. Convective-reactive Proton-¹²C Combustion in Sakurai's Object (V4334 Sagittarii) and Implications for the Evolution and Yields from the First Generations of Stars. *ApJ* **2011**, *727*, 89, [arXiv:astro-ph.SR/1002.2241]. <https://doi.org/10.1088/0004-637X/727/2/89>.
113. Herwig, F.; Blöcker, T.; Langer, N.; Driebe, T. On the formation of hydrogen-deficient post-AGB stars. *A&A* **1999**, *349*, L5–L8, [arXiv:astro-ph/astro-ph/9908108]. <https://doi.org/10.48550/arXiv.astro-ph/9908108>.
114. Lawlor, T.M.; MacDonald, J. Sakurai's Object, V605 Aquilae, and FG Sagittae: An Evolutionary Sequence Revealed. *ApJ* **2003**, *583*, 913–922. <https://doi.org/10.1086/345411>.
115. Lawlor, T.M.; MacDonald, J. The mass of helium in white dwarf stars and the formation and evolution of hydrogen-deficient post-AGB stars. *MNRAS* **2006**, *371*, 263–282, [arXiv:astro-ph/astro-ph/0605747]. <https://doi.org/10.1111/j.1365-2966.2006.10641.x>.
116. Althaus, L.G.; Serenelli, A.M.; Panei, J.A.; Córscico, A.H.; García-Berro, E.; Scóccola, C.G. The formation and evolution of hydrogen-deficient post-AGB white dwarfs: The emerging chemical profile and the expectations for the PG 1159-DB-DQ evolutionary connection. *A&A* **2005**, *435*, 631–648, [arXiv:astro-ph/astro-ph/0502005]. <https://doi.org/10.1051/0004-6361:20041965>.

117. Battich, T.; Althaus, L.G.; Córscico, A.H. On the formation of hydrogen-deficient low-mass white dwarfs. *A&A* **2020**, *638*, A30, [arXiv:astro-ph.SR/2003.13602]. <https://doi.org/10.1051/0004-6361/202037743>.
118. Miller Bertolami, M.M. New models for the evolution of post-asymptotic giant branch stars and central stars of planetary nebulae. *A&A* **2016**, *588*, A25, [arXiv:astro-ph.SR/1512.04129]. <https://doi.org/10.1051/0004-6361/201526577>.
119. Lawlor, T.M. A closer look at low-mass post-AGB late thermal pulses. *MNRAS* **2023**, *519*, 5373–5383, [arXiv:astro-ph.SR/2302.04929]. <https://doi.org/10.1093/mnras/stad042>.
120. Miller Bertolami, M.M. Formación de estrellas deficientes en hidrógeno por medio de flashes tardíos del helio . PhD thesis, Universidad Nacional de La Plata, Argentina, 2009.
121. Miller Bertolami, M.M.; Althaus, L.G.; Córscico, A.H. The formation of DA white dwarfs with thin Hydrogen envelopes through a late thermal pulse. *Boletín de la Asociación Argentina de Astronomía La Plata Argentina* **2005**, *48*, 185–191.
122. Lawlor, T.M. New models for the rapid evolution of the central star of the Stingray Nebula. *MNRAS* **2021**, *504*, 667–677, [arXiv:astro-ph.SR/2104.00733]. <https://doi.org/10.1093/mnras/stab890>.
123. Blöcker, T. H- and He-burning Central Stars and the Evolution to White Dwarfs (invited review). In Proceedings of the Planetary Nebulae: Their Evolution and Role in the Universe; Kwok, S.; Dopita, M.; Sutherland, R., Eds., 2003, Vol. 209, p. 101, [arXiv:astro-ph/astro-ph/0207161]. <https://doi.org/10.48550/arXiv.astro-ph/0207161>.
124. Althaus, L.G.; Miller Bertolami, M.M.; Córscico, A.H.; García-Berro, E.; Gil-Pons, P. The formation of DA white dwarfs with thin hydrogen envelopes. *A&A* **2005**, *440*, L1–L4, [arXiv:astro-ph/astro-ph/0507415]. <https://doi.org/10.1051/0004-6361:200500159>.
125. Herwig, F. Internal mixing and surface abundance of [WC]-CSPN. *Ap&SS* **2001**, *275*, 15–26, [arXiv:astro-ph/astro-ph/9912353]. <https://doi.org/10.48550/arXiv.astro-ph/9912353>.
126. Herwig, F.; Woodward, P.R.; Lin, P.H.; Knox, M.; Fryer, C. Global Non-spherical Oscillations in Three-dimensional 4π Simulations of the H-ingestion Flash. *ApJL* **2014**, *792*, L3, [arXiv:astro-ph.SR/1310.4584]. <https://doi.org/10.1088/2041-8205/792/1/L3>.
127. Woodward, P.R.; Herwig, F.; Lin, P.H. Hydrodynamic Simulations of H Entrainment at the Top of He-shell Flash Convection. *ApJ* **2015**, *798*, 49. <https://doi.org/10.1088/0004-637X/798/1/49>.
128. Burbidge, E.M.; Burbidge, G.R.; Fowler, W.A.; Hoyle, F. Synthesis of the Elements in Stars. *Reviews of Modern Physics* **1957**, *29*, 547–650. <https://doi.org/10.1103/RevModPhys.29.547>.
129. Stephens, D.; Herwig, F.; Woodward, P.; Denissenkov, P.; Androssy, R.; Mao, H. 3D1D hydro-nucleosynthesis simulations - I. Advective-reactive post-processing method and its application to H ingestion into He-shell flash convection in rapidly accreting white dwarfs. *MNRAS* **2021**, *504*, 744–760, [arXiv:astro-ph.SR/2001.10969]. <https://doi.org/10.1093/mnras/stab500>.
130. Althaus, L.G.; Córscico, A.H.; Isern, J.; García-Berro, E. Evolutionary and pulsational properties of white dwarf stars. *A&ARev* **2010**, *18*, 471–566, [arXiv:astro-ph.SR/1007.2659]. <https://doi.org/10.1007/s00159-010-0033-1>.
131. Althaus, L.G.; Córscico, A.H.; Uzundag, M.; Vučković, M.; Baran, A.S.; Bell, K.J.; Camisassa, M.E.; Calcaferro, L.M.; De Gerónimo, F.C.; Kepler, S.O.; et al. About the existence of warm H-rich pulsating white dwarfs. *A&A* **2020**, *633*, A20, [arXiv:astro-ph.SR/1911.02442]. <https://doi.org/10.1051/0004-6361/201936346>.
132. Miller Bertolami, M.M.; Althaus, L.G.; Córscico, A.H. On the Formation of DA White Dwarfs with low Hydrogen Contents: Preliminary Results. In Proceedings of the 20th European White Dwarf Workshop; Tremblay, P.E.; Gaensicke, B.; Marsh, T., Eds., 2017, Vol. 509, *Astronomical Society of the Pacific Conference Series*, p. 435, [arXiv:astro-ph.SR/1609.08683]. <https://doi.org/10.48550/arXiv.1609.08683>.
133. Herwig, F. Evolution of Asymptotic Giant Branch Stars. *ARA&A* **2005**, *43*, 435–479. <https://doi.org/10.1146/annurev.astro.43.072103.150600>.
134. Clayton, G.C.; De Marco, O. The Evolution of the Final Helium Shell Flash Star V605 Aquilae From 1917 to 1997. *AJ* **1997**, *114*, 2679. <https://doi.org/10.1086/118678>.
135. Duerbeck, H.W.; Hazen, M.L.; Misch, A.A.; Seitter, W.C. The light curve of V605 Aql - the ‘older twin’ of Sakurai’s Object. *Ap&SS* **2002**, *279*, 183–186, [arXiv:astro-ph/astro-ph/0102347]. <https://doi.org/10.48550/arXiv.astro-ph/0102347>.
136. Lechner, M.F.M.; Kimeswenger, S. The progenitor of the “born-again” core V605 Aql and the relation to its younger twin V4334 Sgr. *A&A* **2004**, *426*, 145–149, [arXiv:astro-ph/astro-ph/0406507]. <https://doi.org/10.1051/0004-6361:20040387>.
137. Clayton, G.C.; Kerber, F.; Pirzkal, N.; De Marco, O.; Crowther, P.A.; Fedrow, J.M. V605 Aquilae: The Older Twin of Sakurai’s Object. *ApJL* **2006**, *646*, L69–L72, [arXiv:astro-ph/astro-ph/0606257]. <https://doi.org/10.1086/506593>.
138. Offner, S.S.R.; Moe, M.; Kratter, K.M.; Sadavoy, S.I.; Jensen, E.L.N.; Tobin, J.J. The Origin and Evolution of Multiple Star Systems. In Proceedings of the Protostars and Planets VII; Inutsuka, S.; Aikawa, Y.; Muto, T.; Tomida, K.; Tamura, M., Eds., 2023, Vol. 534, *Astronomical Society of the Pacific Conference Series*, p. 275, [arXiv:astro-ph.SR/2203.10066]. <https://doi.org/10.48550/arXiv.2203.10066>.
139. Miller Bertolami, M.M.; Battich, T.; Córscico, A.H.; Althaus, L.G.; Wachlin, F.C. An evolutionary channel for CO-rich and pulsating He-rich subdwarfs. *MNRAS* **2022**, *511*, L60–L65, [arXiv:astro-ph.SR/2202.05635]. <https://doi.org/10.1093/mnras/lsab134>.
140. van Hoof, P.A.M.; Kimeswenger, S.; Van de Steene, G.; Avison, A.; Zijlstra, A.; Guzman-Ramirez, L.; Herwig, F.; Hajduk, M. The Real-Time Evolution of V4334 Sgr. *Galaxies* **2018**, *6*, 79. <https://doi.org/10.3390/galaxies6030079>.
141. Weidmann, W.A.; Gamen, R. Central stars of planetary nebulae: New spectral classifications and catalogue. *A&A* **2011**, *526*, A6, [arXiv:astro-ph.GA/1010.5376]. <https://doi.org/10.1051/0004-6361/200913984>.

142. Cunningham, T.; Tremblay, P.E.; Gentile Fusillo, N.P.; Hollands, M.; Cukanovaite, E. From hydrogen to helium: the spectral evolution of white dwarfs as evidence for convective mixing. *MNRAS* **2020**, *492*, 3540–3552, [arXiv:astro-ph.SR/1911.00014]. <https://doi.org/10.1093/mnras/stz3638>.
143. Bédard, A. The spectral evolution of white dwarfs: where do we stand? *Ap&SS* **2024**, *369*, 43, [arXiv:astro-ph.SR/2405.01268]. <https://doi.org/10.1007/s10509-024-04307-5>.
144. Romero, A.D.; Córscico, A.H.; Althaus, L.G.; Kepler, S.O.; Castanheira, B.G.; Miller Bertolami, M.M. Toward ensemble asteroseismology of ZZ Ceti stars with fully evolutionary models. *MNRAS* **2012**, *420*, 1462–1480, [arXiv:astro-ph.SR/1109.6682]. <https://doi.org/10.1111/j.1365-2966.2011.20134.x>.
145. Romero, A.D.; Kepler, S.O.; Hermes, J.J.; Amaral, L.A.; Uzundag, M.; Bognár, Z.; Bell, K.J.; VanWyngarden, M.; Baran, A.; Pelisoli, I.; et al. Discovery of 74 new bright ZZ Ceti stars in the first three years of TESS. *MNRAS* **2022**, *511*, 1574–1590, [arXiv:astro-ph.SR/2201.04158]. <https://doi.org/10.1093/mnras/stac093>.
146. Althaus, L.G.; Camisassa, M.E.; Miller Bertolami, M.M.; Córscico, A.H.; García-Berro, E. White dwarf evolutionary sequences for low-metallicity progenitors: The impact of third dredge-up. *A&A* **2015**, *576*, A9, [arXiv:astro-ph.SR/1502.03882]. <https://doi.org/10.1051/0004-6361/201424922>.
147. Reindl, N.; Rauch, T.; Miller Bertolami, M.M.; Todt, H.; Werner, K. Breaking news from the HST: the central star of the Stingray Nebula is now returning towards the AGB. *MNRAS* **2017**, *464*, L51–L55, [arXiv:astro-ph.SR/1609.07113]. <https://doi.org/10.1093/mnrasl/slw175>.
148. Miller Bertolami, M.M.; Rohrmann, R.D.; Granada, A.; Althaus, L.G. NSV 11749, an Elder Sibling of the Born-again Stars V605 Aql and V4334 Sgr? *ApJL* **2011**, *743*, L33, [arXiv:astro-ph.SR/1111.2333]. <https://doi.org/10.1088/2041-8205/743/2/L33>.
149. Toalá, J.A.; Jiménez-Hernández, P.; Rodríguez-González, J.B.; Estrada-Dorado, S.; Guerrero, M.A.; Gómez-González, V.M.A.; Ramos-Larios, G.; García-Hernández, D.A.; Todt, H. Carbon dust in the evolved born-again planetary nebulae A 30 and A 78. *MNRAS* **2021**, *503*, 1543–1556, [arXiv:astro-ph.GA/2102.12884]. <https://doi.org/10.1093/mnras/stab593>.
150. Guerrero, M.A.; Manchado, A. The Chemical Abundances of the Hydrogen-poor Planetary Nebulae A30 and A58. *ApJ* **1996**, *472*, 711. <https://doi.org/10.1086/178101>.
151. Montoro-Molina, B.; Guerrero, M.A.; Toalá, J.A. Spatially resolved spectroscopic investigation of the born-again planetary nebula A 78. *MNRAS* **2023**, *526*, 4359–4377, [arXiv:astro-ph.SR/2309.08242]. <https://doi.org/10.1093/mnras/stad2803>.
152. Fang, X.; Guerrero, M.A.; Marquez-Lugo, R.A.; Toalá, J.A.; Arthur, S.J.; Chu, Y.H.; Blair, W.P.; Gruendl, R.A.; Hamann, W.R.; Oskinova, L.M.; et al. Expansion of Hydrogen-poor Knots in the Born-again Planetary Nebulae A30 and A78. *ApJ* **2014**, *797*, 100, [arXiv:astro-ph.SR/1410.3872]. <https://doi.org/10.1088/0004-637X/797/2/100>.
153. Manick, R.; Miszalski, B.; McBride, V. A radial velocity survey for post-common-envelope Wolf-Rayet central stars of planetary nebulae: first results and discovery of the close binary nucleus of NGC 5189. *MNRAS* **2015**, *448*, 1789–1806, [arXiv:astro-ph.SR/1501.03373]. <https://doi.org/10.1093/mnras/stv074>.
154. Nagel, T.; Schuh, S.; Kusterer, D.J.; Stahn, T.; Hügelmeier, S.D.; Dreizler, S.; Gänsicke, B.T.; Schreiber, M.R. SDSS J212531.92-010745.9 - the first definite PG 1159 close binary system. *A&A* **2006**, *448*, L25–L28, [arXiv:astro-ph/astro-ph/0601512]. <https://doi.org/10.1051/0004-6361:200600009>.
155. Schuh, S.; Beeck, B.; Nagel, T. Dynamic masses for the close PG1159 binary SDSSJ212531.92-010745.9. In Proceedings of the Journal of Physics Conference Series. IOP, 2009, Vol. 172, *Journal of Physics Conference Series*, p. 012065, [arXiv:astro-ph/0812.4860]. <https://doi.org/10.1088/1742-6596/172/1/012065>.
156. Bédard, A.; Bergeron, P.; Brassard, P. On the Spectral Evolution of Hot White Dwarf Stars. III. The PG 1159-DO-DB-DQ Evolutionary Channel Revisited. *ApJ* **2022**, *930*, 8, [arXiv:astro-ph.SR/2203.12045]. <https://doi.org/10.3847/1538-4357/ac609d>.
157. Leuenhagen, U.; Koesterke, L.; Hamann, W.R. Analyses of PNNi with [WC] Spectral Type. *Acta Astronomica* **1993**, *43*, 329–335.
158. Koesterke, L.; Hamann, W.R. Spectral analyses of central stars of planetary nebulae of early WC-type NGC 6751 and Sanduleak 3. *A&A* **1997**, *320*, 91–100.
159. Koesterke, L. Spectral analyses of WR-type central stars of planetary nebulae. *Ap&SS* **2001**, *275*, 41–52.
160. Crowther, P.A.; Abbott, J.B.; Hillier, D.J.; De Marco, O. Revised Abundances and Ionizing Fluxes for [WC]-Type PN Central Stars Using Line Blanketed Models. In Proceedings of the Planetary Nebulae: Their Evolution and Role in the Universe; Kwok, S.; Dopita, M.; Sutherland, R., Eds., 2003, Vol. 209, p. 243.
161. Marcolino, W.L.F.; Hillier, D.J.; de Araujo, F.X.; Pereira, C.B. Detailed Far-Ultraviolet to Optical Analysis of Four [WR] Stars. *ApJ* **2007**, *654*, 1068–1086, [arXiv:astro-ph/astro-ph/0609512]. <https://doi.org/10.1086/509316>.
162. Hajduk, M.; Todt, H.; Hamann, W.R.; Borek, K.; van Hoof, P.A.M.; Zijlstra, A.A. The cooling-down central star of the planetary nebula SwSt 1: a late thermal pulse in a massive post-AGB star? *MNRAS* **2020**, *498*, 1205–1220, [arXiv:astro-ph.SR/2009.14616]. <https://doi.org/10.1093/mnras/staa2274>.
163. Toalá, J.A.; Ramos-Larios, G.; Guerrero, M.A.; Todt, H. Hidden IR structures in NGC 40: signpost of an ancient born-again event. *MNRAS* **2019**, *485*, 3360–3369, [arXiv:astro-ph.SR/1902.11219]. <https://doi.org/10.1093/mnras/stz624>.
164. Gómez-González, V.M.A.; Toalá, J.A.; Guerrero, M.A.; Todt, H.; Sabin, L.; Ramos-Larios, G.; Mayya, Y.D. Planetary nebulae with Wolf-Rayet-type central stars - I. The case of the high-excitation NGC 2371. *MNRAS* **2020**, *496*, 959–973, [arXiv:astro-ph.SR/2005.14294]. <https://doi.org/10.1093/mnras/staa1542>.

165. Gómez-González, V.M.A.; Rubio, G.; Toalá, J.A.; Guerrero, M.A.; Sabin, L.; Todt, H.; Gómez-Llanos, V.; Ramos-Larios, G.; Mayya, Y.D. Planetary nebulae with Wolf-Rayet-type central stars - III. A detailed view of NGC 6905 and its central star. *MNRAS* **2022**, *509*, 974–989, [arXiv:astro-ph.SR/2110.09551]. <https://doi.org/10.1093/mnras/stab3042>.
166. Rubio, G.; Toalá, J.A.; Todt, H.; Sabin, L.; Santamaría, E.; Ramos-Larios, G.; Guerrero, M.A. Planetary nebulae with Wolf-Rayet-type central stars - IV. NGC 1501 and its mixing layer. *MNRAS* **2022**, *517*, 5166–5179, [arXiv:astro-ph.SR/2210.09116]. <https://doi.org/10.1093/mnras/stac3011>.
167. Guerrero, M.A.; Ruiz, N.; Hamann, W.R.; Chu, Y.H.; Todt, H.; Schönberner, D.; Oskinova, L.; Gruendl, R.A.; Steffen, M.; Blair, W.P.; et al. Rebirth of X-Ray Emission from the Born-again Planetary Nebula A30. *ApJ* **2012**, *755*, 129, [arXiv:astro-ph.GA/1202.4463]. <https://doi.org/10.1088/0004-637X/755/2/129>.
168. Toalá, J.A.; Guerrero, M.A.; Todt, H.; Hamann, W.R.; Chu, Y.H.; Gruendl, R.A.; Schönberner, D.; Oskinova, L.M.; Marquez-Lugo, R.A.; Fang, X.; et al. The Born-again Planetary Nebula A78: An X-Ray Twin of A30. *ApJ* **2015**, *799*, 67, [arXiv:astro-ph.SR/1411.3837]. <https://doi.org/10.1088/0004-637X/799/1/67>.
169. Hernández-Juárez, D.; Rodríguez, M.; Peña, M. New catalog of distances to planetary nebulae based on Gaia parallaxes and statistical distances. *arXiv e-prints* **2024**, p. arXiv:2403.04606, [arXiv:astro-ph.SR/2403.04606]. <https://doi.org/10.48550/arXiv.2403.04606>.
170. Peña, M.; Rechy-García, J.S.; García-Rojas, J. Galactic kinematics of Planetary Nebulae with [WC] central star. *RMxAA* **2013**, *49*, 87–99, [arXiv:astro-ph.GA/1301.3657]. <https://doi.org/10.48550/arXiv.1301.3657>.
171. Górny, S.K.; Tylenda, R. Evolutionary status of hydrogen-deficient central stars of planetary nebulae. *A&A* **2000**, *362*, 1008–1019.
172. Clayton, G.C. The R Coronae Borealis Stars. *PASP* **1996**, *108*, 225. <https://doi.org/10.1086/133715>.
173. Miranda Marques, B.L.; Monteiro, H.; Aleman, I.; Akras, S.; Todt, H.; Corradi, R.L.M. Analysis of integral field spectroscopy observations of the planetary nebula Hen 2-108 and its central star. *MNRAS* **2023**, *522*, 1049–1070, [arXiv:astro-ph.SR/2306.03201]. <https://doi.org/10.1093/mnras/stad1055>.
174. Werner, K.; Rauch, T. Hubble Space Telescope ultraviolet spectroscopy of the hottest known helium-rich pre-white dwarf KPD 0005+5106. *A&A* **2015**, *583*, A131, [arXiv:astro-ph.SR/1509.08938]. <https://doi.org/10.1051/0004-6361/201527212>.
175. Raghavan, D.; McAlister, H.A.; Henry, T.J.; Latham, D.W.; Marcy, G.W.; Mason, B.D.; Gies, D.R.; White, R.J.; ten Brummelaar, T.A. A Survey of Stellar Families: Multiplicity of Solar-type Stars. *ApJS* **2010**, *190*, 1–42, [arXiv:astro-ph.SR/1007.0414]. <https://doi.org/10.1088/0067-0049/190/1/1>.
176. Tokovinin, A. From Binaries to Multiples. I. Data on F and G Dwarfs within 67 pc of the Sun. *AJ* **2014**, *147*, 86, [arXiv:astro-ph.SR/1401.6825]. <https://doi.org/10.1088/0004-6256/147/4/86>.
177. Eggleton, P. *Evolutionary Processes in Binary and Multiple Stars*; 2006.
178. Postnov, K.A.; Yungelson, L.R. The Evolution of Compact Binary Star Systems. *Living Reviews in Relativity* **2014**, *17*, 3, [arXiv:astro-ph.HE/1403.4754]. <https://doi.org/10.12942/lrr-2014-3>.
179. De Marco, O.; Izzard, R.G. Dawes Review 6: The Impact of Companions on Stellar Evolution. *PASA* **2017**, *34*, e001, [arXiv:astro-ph.SR/1611.03542]. <https://doi.org/10.1017/pasa.2016.52>.
180. Tauris, T.M.; van den Heuvel, E.P.J. *Physics of Binary Star Evolution. From Stars to X-ray Binaries and Gravitational Wave Sources*; 2023. <https://doi.org/10.48550/arXiv.2305.09388>.
181. Bondi, H.; Hoyle, F. On the mechanism of accretion by stars. *MNRAS* **1944**, *104*, 273. <https://doi.org/10.1093/mnras/104.5.273>.
182. Mohamed, S.; Podsiadlowski, P. Wind Roche-Lobe Overflow: a New Mass-Transfer Mode for Wide Binaries. In Proceedings of the 15th European Workshop on White Dwarfs; Napiwotzki, R.; Burleigh, M.R., Eds., 2007, Vol. 372, *Astronomical Society of the Pacific Conference Series*, p. 397.
183. Paczyński, B. Evolutionary Processes in Close Binary Systems. *ARA&A* **1971**, *9*, 183. <https://doi.org/10.1146/annurev.aa.09.090171.001151>.
184. Paczynski, B. Common Envelope Binaries. In Proceedings of the Structure and Evolution of Close Binary Systems; Eggleton, P.; Mitton, S.; Whelan, J., Eds., 1976, Vol. 73, p. 75.
185. Zahn, J.P. The dynamical tide in close binaries. *A&A* **1975**, *41*, 329–344.
186. Preece, H.P.; Hamers, A.S.; Neunteufel, P.G.; Schaefer, A.L.; Tout, C.A. The Equilibrium Tide: An Updated Prescription for Population Synthesis Codes. *ApJ* **2022**, *933*, 25, [arXiv:astro-ph.SR/2206.06068]. <https://doi.org/10.3847/1538-4357/ac6fe3>.
187. Esseldeurs, M.; Mathis, S.; Decin, L. Tidal Dissipation in Evolved Low and Intermediate Mass Stars. *arXiv e-prints* **2024**, p. arXiv:2407.10573, [arXiv:astro-ph.SR/2407.10573]. <https://doi.org/10.48550/arXiv.2407.10573>.
188. Pavlovskii, K.; Ivanova, N. Mass transfer from giant donors. *MNRAS* **2015**, *449*, 4415–4427, [arXiv:astro-ph.SR/1410.5109]. <https://doi.org/10.1093/mnras/stv619>.
189. Eggleton, P. Close Binary Stars. In *Encyclopedia of Astronomy and Astrophysics*; Murdin, P., Ed.; 2000; p. 1624. <https://doi.org/10.1888/0333750888/1624>.
190. Chen, Z.; Blackman, E.G.; Nordhaus, J.; Frank, A.; Carroll-Nellenback, J. Wind-accelerated orbital evolution in binary systems with giant stars. *MNRAS* **2018**, *473*, 747–756, [arXiv:astro-ph.SR/1705.01998]. <https://doi.org/10.1093/mnras/stx2335>.
191. Hall, P.D.; Tout, C.A.; Izzard, R.G.; Keller, D. Planetary nebulae after common-envelope phases initiated by low-mass red giants. *MNRAS* **2013**, *435*, 2048–2059, [arXiv:astro-ph.SR/1307.8023]. <https://doi.org/10.1093/mnras/stt1422>.

192. Ivanova, N.; Justham, S.; Chen, X.; De Marco, O.; Fryer, C.L.; Gaburov, E.; Ge, H.; Glebbeek, E.; Han, Z.; Li, X.D.; et al. Common envelope evolution: where we stand and how we can move forward. *A&ARev* **2013**, *21*, 59, [arXiv:astro-ph.HE/1209.4302]. <https://doi.org/10.1007/s00159-013-0059-2>.
193. Jones, D. Observational Constraints on the Common Envelope Phase. In *Reviews in Frontiers of Modern Astrophysics; From Space Debris to Cosmology*; 2020; pp. 123–153. https://doi.org/10.1007/978-3-030-38509-5_5.
194. Jones, D. Binary Central Stars of Planetary Nebulae. *Galaxies* **2020**, *8*, 28. <https://doi.org/10.3390/galaxies8020028>.
195. Webbink, R.F. Double white dwarfs as progenitors of R Coronae Borealis stars and type I supernovae. *ApJ* **1984**, *277*, 355–360. <https://doi.org/10.1086/161701>.
196. Saio, H.; Jeffery, C.S. Merged binary white dwarf evolution: rapidly accreting carbon-oxygen white dwarfs and the progeny of extreme helium stars. *MNRAS* **2002**, *333*, 121–132. <https://doi.org/10.1046/j.1365-8711.2002.05384.x>.
197. Clayton, G.C.; Geballe, T.R.; Herwig, F.; Fryer, C.; Asplund, M. Very Large Excesses of ^{18}O in Hydrogen-deficient Carbon and R Coronae Borealis Stars: Evidence for White Dwarf Mergers. *ApJ* **2007**, *662*, 1220–1230, [arXiv:astro-ph/astro-ph/0703453]. <https://doi.org/10.1086/518307>.
198. Asplund, M.; Gustafsson, B.; Lambert, D.L.; Rao, N.K. The R Coronae Borealis stars - atmospheres and abundances. *A&A* **2000**, *353*, 287–310.
199. De Marco, O.; Clayton, G.C.; Herwig, F.; Pollacco, D.L.; Clark, J.S.; Kilkenny, D. What Are the Hot R Coronae Borealis Stars? *AJ* **2002**, *123*, 3387–3408, [arXiv:astro-ph/astro-ph/0203136]. <https://doi.org/10.1086/340569>.
200. Weiss, A. Evolutionary models for R CrB stars. *A&A* **1987**, *185*, 165–177.
201. Schwab, J. Evolutionary Models for R Coronae Borealis Stars. *ApJ* **2019**, *885*, 27, [arXiv:astro-ph.SR/1909.02569]. <https://doi.org/10.3847/1538-4357/ab425d>.
202. Rauch, T.; Koeppen, J.; Werner, K. Spectral analysis of the planetary nebula K 1-27 and its very hot hydrogen-deficient central star. *A&A* **1994**, *286*, 543–554.
203. Rauch, T.; Koeppen, J.; Werner, K. Spectral analysis of the multiple-shell planetary nebula LoTr4 and its very hot hydrogen-deficient central star. *A&A* **1996**, *310*, 613–628.
204. García-Rojas, J.; Peña, M.; Peimbert, A. Faint recombination lines in Galactic PNe with a [WC] nucleus. *A&A* **2009**, *496*, 139–152, [arXiv:astro-ph/0812.3049]. <https://doi.org/10.1051/0004-6361:200811185>.
205. Danehkar, A. 3D spatio-kinematic modelling of Abell 48, a planetary nebula around a Wolf-Rayet [WN] star. *MNRAS* **2022**, *511*, 1022–1028, [arXiv:astro-ph.SR/2112.12043]. <https://doi.org/10.1093/mnras/stab3735>.
206. Mohery, M.; Ali, A.; Khames, A.A.; Snaid, S.; Mindil, A. Exploring the high abundance discrepancy in the planetary nebula IC 4663. *Frontiers in Astronomy and Space Sciences* **2023**, *10*, 1322980. <https://doi.org/10.3389/fspas.2023.1322980>.
207. De Marco, O. [WC] and PG 1159 Central Stars of Planetary Nebulae: The Need for an Alternative to the Born-Again Scenario. In *Proceedings of the Hydrogen-Deficient Stars*; Werner, A.; Rauch, T., Eds., 2008, Vol. 391, *Astronomical Society of the Pacific Conference Series*, p. 209, [arXiv:astro-ph/0711.2461]. <https://doi.org/10.48550/arXiv.0711.2461>.
208. De Marco, O.; Soker, N. A New Look at the Evolution of Wolf-Rayet Central Stars of Planetary Nebulae. *PASP* **2002**, *114*, 602–611, [arXiv:astro-ph/astro-ph/0204230]. <https://doi.org/10.1086/341691>.
209. Byrne, C.M.; Jeffery, C.S.; Tout, C.A.; Hu, H. The effects of diffusion in hot subdwarf progenitors from the common envelope channel. *MNRAS* **2018**, *475*, 4728–4738, [arXiv:astro-ph.SR/1802.00436]. <https://doi.org/10.1093/mnras/sty158>.
210. Lau, H.H.B.; De Marco, O.; Liu, X.W. V605 Aquilae: a born-again star, a nova or both? *MNRAS* **2011**, *410*, 1870–1876, [arXiv:astro-ph.SR/1009.3138]. <https://doi.org/10.1111/j.1365-2966.2010.17568.x>.
211. Gonzalez, G.; Lambert, D.L.; Wallerstein, G.; Rao, N.K.; Smith, V.V.; McCarthy, J.K. FG Sagittae: A Newborn R Coronae Borealis Star? *ApJS* **1998**, *114*, 133–149. <https://doi.org/10.1086/313068>.
212. van Genderen, A.M.; Gautschy, A. Deductions from the reconstructed evolutionary and pulsational history of FG Sagittae. *A&A* **1995**, *294*, 453–468.
213. Jeffery, C.S.; Schönberner, D. Stellar archaeology: the evolving spectrum of FG Sagittae. *A&A* **2006**, *459*, 885–899, [arXiv:astro-ph/astro-ph/0608542]. <https://doi.org/10.1051/0004-6361:20047075>.
214. Nakano, S.; Sakurai, Y.; Hazen, M.; McNaught, R.H.; Benetti, S.; Duerbeck, H.W.; Cappellaro, E.; Leibundgut, B. Novalike Variable in Sagittarius. *IAU Circ.* **1996**, 6322, 1.
215. Benetti, S.; Duerbeck, H.W.; Seitter, W.C.; Harrison, T.; Hoff, W. Novalike Variable in Sagittarius. *IAU Circ.* **1996**, 6325, 1.
216. Duerbeck, H.W.; Pollacco, D.; Verbunt, F.; Geertsema, G.; van den Berg, M.; Green, D.W.E. Novalike Variable in Sagittarius. *IAU Circ.* **1996**, 6328, 1.
217. Duerbeck, H.W.; Benetti, S. Sakurai's Object—A Possible Final Helium Flash in a Planetary Nebula Nucleus. *ApJL* **1996**, *468*, L111. <https://doi.org/10.1086/310241>.
218. Duerbeck, H.W.; Benetti, S.; Gautschy, A.; van Genderen, A.M.; Kemper, C.; Liller, W.; Thomas, T. The Final Helium Flash Object Sakurai: Photometric Behavior and Physical Characteristics. *AJ* **1997**, *114*, 1657. <https://doi.org/10.1086/118595>.
219. Duerbeck, H.W.; Liller, W.; Sterken, C.; Benetti, S.; van Genderen, A.M.; Arts, J.; Kurk, J.D.; Janson, M.; Voskes, T.; Brogt, E.; et al. The Rise and Fall of V4334 Sagittarii (Sakurai's Object). *AJ* **2000**, *119*, 2360–2375, [arXiv:astro-ph/astro-ph/0001534]. <https://doi.org/10.1086/301349>.
220. Asplund, M.; Gustafsson, B.; Lambert, D.L.; Kameswara Rao, N. A stellar endgame - the born-again Sakurai's object. *A&A* **1997**, *321*, L17–L20, [arXiv:astro-ph/astro-ph/9704005]. <https://doi.org/10.48550/arXiv.astro-ph/9704005>.

221. Asplund, M.; Lambert, D.L.; Kipper, T.; Pollacco, D.; Shetrone, M.D. The rapid evolution of the born-again giant Sakurai's object. *A&A* **1999**, *343*, 507–518, [arXiv:astro-ph/astro-ph/9811208]. <https://doi.org/10.48550/arXiv.astro-ph/9811208>.
222. Kerber, F.; Köppen, J.; Roth, M.; Trager, S.C. The hidden past of Sakurai's object. Stellar properties before the final helium flash. *A&A* **1999**, *344*, L79–L82.
223. Pollacco, D. The planetary nebula surrounding the final thermal pulse object V4334 Sagittarii. *MNRAS* **1999**, *304*, 127–134. <https://doi.org/10.1046/j.1365-8711.1999.02300.x>.
224. Hajduk, M.; Gesicki, K.; van Hoof, P.A.M.; Lopez, J.A.; Zijlstra, A.A. Studying the Old Planetary Nebula of V4334 Sgr. In Proceedings of the Hydrogen-Deficient Stars; Werner, A.; Rauch, T., Eds., 2008, Vol. 391, *Astronomical Society of the Pacific Conference Series*, p. 163.
225. Hajduk, M.; Zijlstra, A.A.; Herwig, F.; van Hoof, P.A.M.; Kerber, F.; Kimeswenger, S.; Pollacco, D.L.; Evans, A.; Lopéz, J.A.; Bryce, M.; et al. The Real-Time Stellar Evolution of Sakurai's Object. *Science* **2005**, *308*, 231–233. <https://doi.org/10.1126/science.1108953>.
226. van Hoof, P.A.M.; Hajduk, M.; Zijlstra, A.A.; Herwig, F.; Evans, A.; van de Steene, G.C.; Kimeswenger, S.; Kerber, F.; Eyres, S.P.S. The onset of photoionization in Sakurai's Object (V4334 Sagittarii). *A&A* **2007**, *471*, L9–L12, [arXiv:astro-ph/0706.3857]. <https://doi.org/10.1051/0004-6361:20077932>.
227. Hajduk, M.; van Hoof, P.A.M.; Zijlstra, A.A.; Van de Steene, G.; Kimeswenger, S.; Barría, D.; Tafuya, D.; Toalá, J.A. Non-thermal radio emission in Sakurai's Object. *arXiv e-prints* **2024**, p. arXiv:2407.18020, [arXiv:astro-ph.SR/2407.18020]. <https://doi.org/10.48550/arXiv.2407.18020>.
228. Lundmark, K. Nova Aquilae No. 4. *PASP* **1921**, *33*, 314. <https://doi.org/10.1086/123122>.
229. Ford, H.C. V605 Aquilae: a Nova-Like Variable in an Old Planetary Nebula. *ApJ* **1971**, *170*, 547. <https://doi.org/10.1086/151239>.
230. Hinkle, K.H.; Lebzelter, T.; Joyce, R.R.; Ridgway, S.; Close, L.; Hron, J.; Andre, K. Imaging ejecta from the final flash star V605 Aquilae. *A&A* **2008**, *479*, 817–826. <https://doi.org/10.1051/0004-6361:20077738>.
231. Montoro-Molina, B.; Guerrero, M.A.; Toalá, J.A.; Rodríguez-González, J.B. Spectral Variability of the Born-again Ejecta in A 58. *ApJ* **2022**, *934*, 18, [arXiv:astro-ph.SR/2206.10203]. <https://doi.org/10.3847/1538-4357/ac771b>.
232. Montoro-Molina, B.; Tafuya, D.; Guerrero, M.A.; Toalá, J.A.; Santamaría, E. Optical tomography of the born-again ejecta of A 58. *A&A* **2024**, *684*, A107, [arXiv:astro-ph.SR/2401.09844]. <https://doi.org/10.1051/0004-6361/202348528>.
233. Wackerling, L.R. A catalogue of early-type stars whose spectra have shown emission lines. *MNRAS* **1970**, *73*, 153.
234. Parthasarathy, M.; Garcia-Lario, P.; Pottasch, S.R.; Machado, A.; Clavel, J.; de Martino, D.; van de Steene, G.C.M.; Sahu, K.C. SAO 244567 : a post-AGB star which has turned into a planetary nebula within the last 40 years. *A&A* **1993**, *267*, L19–L22.
235. Parthasarathy, M.; Garcia-Lario, P.; de Martino, D.; Pottasch, S.R.; Kilkenny, D.; Martinez, P.; Sahu, K.C.; Reddy, B.E.; Sewell, B.T. Fading and variations in the spectrum of the central star of the very young planetary nebula SAO 244567 (Hen 1357). *A&A* **1995**, *300*, L25.
236. Reindl, N.; Rauch, T.; Parthasarathy, M.; Werner, K.; Kruk, J.W.; Hamann, W.R.; Sander, A.; Todt, H. The rapid evolution of the exciting star of the Stingray nebula. *A&A* **2014**, *565*, A40, [arXiv:astro-ph.SR/1403.6056]. <https://doi.org/10.1051/0004-6361/201323189>.
237. Schaefer, B.E.; Edwards, Z.I. Photometry of the Stingray Nebula (V839 Ara) from 1889 TO 2015 across the Ionization of Its Planetary Nebula. *ApJ* **2015**, *812*, 133, [arXiv:astro-ph.SR/1509.01202]. <https://doi.org/10.1088/0004-637X/812/2/133>.
238. Peña, M.; Parthasarathy, M.; Ruiz-Escobedo, F.; Manick, R. Evolution of Hen 3-1357, the Stingray Nebula. *MNRAS* **2022**, *515*, 1459–1468, [arXiv:astro-ph.SR/2206.10663]. <https://doi.org/10.1093/mnras/stac1750>.
239. Balick, B.; Guerrero, M.A.; Ramos-Larios, G. The Decline and Fall of the Youngest Planetary Nebula. *ApJ* **2021**, *907*, 104, [arXiv:astro-ph.SR/2009.01701]. <https://doi.org/10.3847/1538-4357/abcc61>.
240. Evans, A.; van Loon, J.T.; Zijlstra, A.A.; Pollacco, D.; Smalley, B.; Tyne, V.H.; Eyres, S.P.S. CK Vul: reborn perhaps, but not hibernating. *MNRAS* **2002**, *332*, L35–L38. <https://doi.org/10.1046/j.1365-8711.2002.05476.x>.
241. Lawlor, T.M. A new model for V838 Monocerotis: a born-again object including an episode of accretion. *MNRAS* **2005**, *361*, 695–700. <https://doi.org/10.1111/j.1365-2966.2005.09230.x>.
242. Tylenda, R.; Soker, N.; Szczerba, R. On the progenitor of V838 Monocerotis. *A&A* **2005**, *441*, 1099–1109, [arXiv:astro-ph/astro-ph/0412183]. <https://doi.org/10.1051/0004-6361:20042485>.
243. Tylenda, R.; Soker, N. Eruptions of the V838 Mon type: stellar merger versus nuclear outburst models. *A&A* **2006**, *451*, 223–236, [arXiv:astro-ph/astro-ph/0509379]. <https://doi.org/10.1051/0004-6361:20054201>.
244. Bond, H.E.; Kasliwal, M.M. NSV 11749: Symbiotic Nova, Not a Born-Again Red Giant. *PASP* **2012**, *124*, 1262, [arXiv:astro-ph.SR/1210.6404]. <https://doi.org/10.1086/668861>.
245. Tylenda, R.; Kamiński, T.; Smolec, R. Nova 1670 (CK Vulpeculae) was a merger of a red giant with a helium white dwarf. *A&A* **2024**, *685*, A49, [arXiv:astro-ph.SR/2312.07433]. <https://doi.org/10.1051/0004-6361/202244896>.
246. Pastorello, A.; Mason, E.; Taubenberger, S.; Fraser, M.; Cortini, G.; Tomasella, L.; Botticella, M.T.; Elias-Rosa, N.; Kotak, R.; Smartt, S.J.; et al. Luminous red novae: Stellar mergers or giant eruptions? *A&A* **2019**, *630*, A75, [arXiv:astro-ph.SR/1906.00812]. <https://doi.org/10.1051/0004-6361/201935999>.
247. Peña, M.; Stasińska, G.; Medina, S. Galactic planetary nebulae with Wolf-Rayet nuclei. II. A consistent observational data set. *A&A* **2001**, *367*, 983–994, [arXiv:astro-ph/astro-ph/0101523]. <https://doi.org/10.1051/0004-6361:20000497>.
248. Peña, M. The Low Excitation Planetary Nebulae HuDo 1 and HuBi 1 and their [WC10] Central Stars. *RMxAA* **2005**, *41*, 423–433, [arXiv:astro-ph/astro-ph/0506428]. <https://doi.org/10.48550/arXiv.astro-ph/0506428>.

-
249. Toalá, J.A.; Lora, V.; Montoro-Molina, B.; Guerrero, M.A.; Esquivel, A. Formation and fate of the born-again planetary nebula HuBi 1. *MNRAS* **2021**, *505*, 3883–3891, [arXiv:astro-ph.SR/2103.11503]. <https://doi.org/10.1093/mnras/stab1592>.

Disclaimer/Publisher’s Note: The statements, opinions and data contained in all publications are solely those of the individual author(s) and contributor(s) and not of MDPI and/or the editor(s). MDPI and/or the editor(s) disclaim responsibility for any injury to people or property resulting from any ideas, methods, instructions or products referred to in the content.